ASC

ASTRO
SCIENCES
CENTER

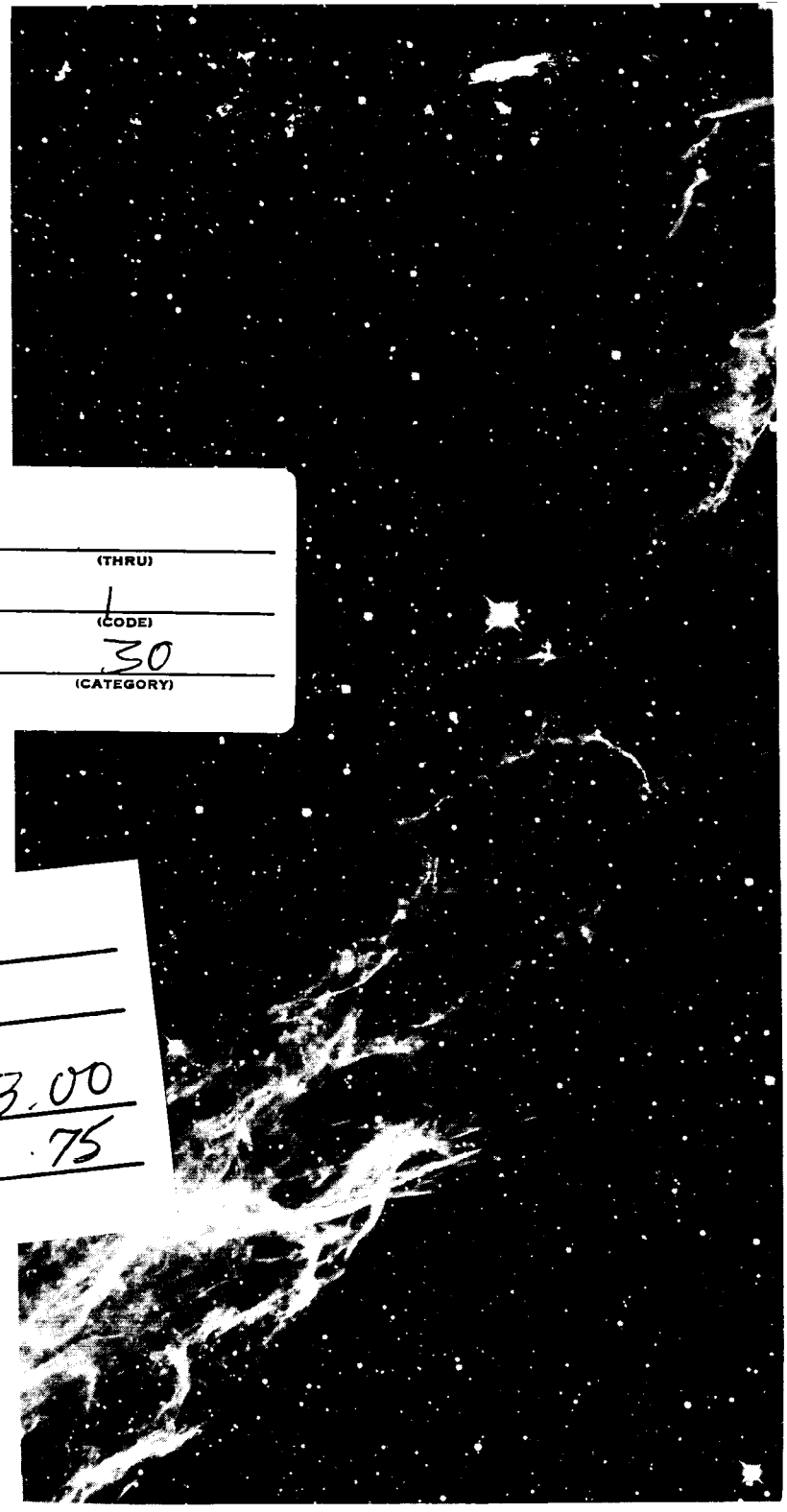

Report No. T-12

AN ANALYSIS OF GRAVITY ASSISTED TRAJECTORIES IN THE ECLIPTIC PLANE

Report No. T-12

AN ANALYSIS OF GRAVITY ASSISTED TRAJECTORIES IN THE ECLIPTIC PLANE

by

J. Niehoff

Astro Sciences Center
of
IIT Research Institute
Chicago, Illinois

for

Lunar and Planetary Programs
National Aeronautics and Space Administration
Washington, D. C. 20546

Contract No. NASr-65(06)

APPROVED:

C. A. Stone, Director
Astro Sciences Center

May 25, 1965

ABSTRACT

34460

A parametric trajectory study of gravity assisted Earth launched trajectories has been conducted. A two-dimensional solar system with circular planetary orbits (except Mercury) is assumed. Gravity assist is restricted to one body between launch and target intercept. Analytical expressions and results are presented for maximum velocity and energy changes available to a spacecraft through gravity assist. A review of the Earth-Venus-Mercury mission is considered after which primary emphasis is placed upon Jupiter, both as a target and as a gravity assisting body. Jupiter fly-bys are found to be attractive for solar probe missions and flights to the outer planets. Included in the results of the study are several examples of launch opportunities for gravity assisted trajectories.

Author

ACKNOWLEDGEMENTS

The author acknowledges the contributions of Dr. James Witting, Mr. Alan Friedlander and Mr. Fran Narin. Dr. Witting's and Mr. Friedlander's contributions to the derivation of the analytical maximum expressions were invaluable. Mr. Narin was instrumental in the organization of the study effort. The comments and criticisms of the Astro Sciences Center staff were helpful throughout this work.

SUMMARY

AN ANALYSIS OF GRAVITY ASSISTED TRAJECTORIES IN THE ECLIPTIC PLANE

The Astro Sciences Center of IIT Research Institute is performing long range planning studies for NASA under Contract No. NASr-65(06). This report is a review of gravity assisted trajectories as a means of reaching target planets. An effort has been made to avoid duplication of similar existing studies. Analytical analyses as well as the more common numerical analyses are considered.

The results are based on a two-dimensional solar system. All planets' orbits were considered circular except Mercury's. Two-body equations of motion, i.e. conic trajectories, were employed to ease the numerical work involved. Only one intermediate gravity assist body was considered between launch and target intercept.

Analytical results indicate, as expected, that Jupiter with its large mass is the most effective planet from the standpoint of performance for gravity assist. The theoretical maximum velocity change from a Jupiter assist is 42.5 km/sec.

The maximum energy change is 584 km^2/sec^2. These values were derived under the assumptions stated above. A summary table contains ordered lists of all the planets with the theoretical maximum velocity and energy changes available from them.

A review of the Earth-Venus-Mercury mission was considered first. This was done to check the numerical approach against a more detailed study (Minovitch 1963) and to establish any further performance benefits of a Venus gravity assist if possible. The results obtained indicate that significant reduction can be made in the ideal velocity through the use of a Venus assist. Using an Atlas-Centaur launch vehicle, for example, injected spacecraft weight is increased from 400 pounds to 1200 pounds for the same 115 day trip to Mercury (at 0.47 AU) with the use of gravity assist at Venus. Even greater savings are realized when Mercury is at its perihelion (0.31 AU). These results agree with the work done by Minovitch (1963). The balance of the study emphasizes missions involving Jupiter. Although some preliminary results of Jupiter assisted trajectories have been published (Hunter 1964), it was felt that further analysis would be helpful. The first missions considered, Earth-Venus-Jupiter and Earth-Mars-Jupiter, utilized gravity assisted trajectories to Jupiter as a target. The use of a Venus assist to reach Jupiter requires more energy and takes longer than a direct* flight from Earth.

* Direct trajectories are defined as proceeding from launch point to target point without the benefit of a gravity assist.

The Mars assist to Jupiter proved to be better than a direct flight but reasonable opportunities for such a mission are scarce, the next one occurring in the early 1980's.

The use of Jupiter for gravity assist to the outer planets is shown to be desirable. The first flight of this type considered was the Earth-Jupiter-Saturn mission. The ideal velocity requirements are low enough to allow payloads on the order of 1500 pounds with a Saturn 1B-Centaur launch vehicle. The same launch vehicle provides only 1000 pounds payload for a direct flight to Saturn. The trip time is about three years and good launch opportunities occur in the late 1970's. This is one of the better gravity assisted missions studied in the report.

Using Jupiter's gravitational field to probe the outer regions of the solar system (20 AU to 50 AU) can provide large improvements in trip time over direct flight. A direct flight to 50 AU with an ideal velocity of 58,000 feet/second takes 30 years. With a Jupiter assist the trip time is reduced to 10.5 years. Further reductions in trip time will probably require the use of thrusted trajectories. It is suggested that the combination of thrusted propulsion and gravity assist may be the ultimate method of reaching these outer regions quickly. The feasibility of such a flight should be determined.

Finally, there is the interesting use of Jupiter for gravity assisted solar probe missions. There are disadvantages to such a path to the Sun. Long trip times, on the order of

three years, decreases spacecraft* reliability and the double traversal of the asteroid belt involves hazards. Nevertheless, when missions to less than 0.1 AU were considered it was found that the only available route with conventional propulsion systems was via a Jupiter fly-by. In addition, the ideal velocity requirements with Jupiter's gravity assist, i.e., 55,000 ft/sec are almost the same whether one wishes to go to 0.1 AU or, in fact, impact the Sun. The ideal velocity for a direct flight to 0.1 AU is about 70,000 feet/second; to reach the apparent surface of the Sun (.005 AU) requires almost 100,000 ft/sec.

---

* Definition and discussion of spacecraft problems, e.g. thermal control, are reserved for separate mission studies.

ORDERED LISTS OF MAXIMUM VELOCITY AND ENERGY CHANGES DUE TO PLANETARY GRAVITY ASSIST

Velocity Change		Energy Change					
Planet	Maximum Velocity Change, km/sec	Planet	Maximum Energy Addition, km^2/sec^2	Perihelion Before, AU	Aphelion Before, AU	Perihelion After, AU	Aphelion After, AU
1. Jupiter	42.6	1. Jupiter	583.7	0.59	Hyperbolic	3.30	Hyperbolic
2. Saturn	25.7	2. Saturn	261.7	0.31	Hyperbolic	6.22	Hyperbolic
3. Neptune	16.8	3. Venus	255.2	0.47	0.77	0.68	1.25
4. Uranus	15.1	4. Earth	239.4	0.58	1.09	0.92	2.12
5. Earth	7.9	5. Mercury	173.7	0.31	0.42	0.31	0.53
6. Venus	7.2	6. Uranus	107.6	0.03	Hyperbolic	13.00	Hyperbolic
7. Pluto	6.9	7. Mars	95.5	1.16	1.51	1.34	2.40
8. Mars	3.6	8. Neptune	91.9	3.26	Hyperbolic	19.86	Hyperbolic
9. Mercury	3.0	9. Pluto	42.1	3.66	100.09	23.85	Hyperbolic

TABLE OF CONTENTS

LIST OF TABLES

LIST OF FIGURES

LIST OF FIGURES (Cont'd)

Report No. T-12

AN ANALYSIS OF GRAVITY ASSISTED TRAJECTORIES IN THE ECLIPTIC PLANE

1. INTRODUCTION

In traveling through the solar system from one planet to another, there sometimes is available the option of flying by a third planet (and fourth, fifth, etc.) before reaching the final objective. The gravitational field of the third planet can affect a significant change on the vehicle's trajectory. This effect is known as a gravity assist. It has been demonstrated that gravity assisted trajectories can offer significant advantages and/or improvements in performance, i.e., VHL*, trip time, VHP and opportunities, over direct trajectories with the same launch vehicle requirements. Hunter (1964) has shown that it is more attractive to do a close fly-by of the Sun by first obtaining a gravity assist from Jupiter than it is to proceed directly to the Sun from Earth. The penalty, in this case, for the gravity assist is a much longer flight time. Another study

* A list of all letters, subscripts and abbreviations is given in Appendix A.

(Minovitch 1963) reports desirable energy requirements and launch opportunities for gravity assisted trajectories including the planets Mercury, Venus, Earth and Mars.

A review of the current literature, including the two articles cited above, indicated a need for further analysis in support of the gravity assist techniques. As a result, this study was conducted to obtain more information on gravity assisted missions including Jupiter, either as a target or an assisting planet. In addition, it was felt that the conclusions of such a study could provide useful guidelines to a more detailed analysis of interesting gravity assisted missions.

The gravity assist technique is equally applicable to both ballistic and thrusted trajectories. This study has been confined to the use of gravity assist with ballistic trajectories, however. The objectives of this report are to 1) review the celestial mechanics of gravity assisted trajectories, 2) determine the advantages and disadvantages of gravity assisted trajectories for the following combinations of bodies:

1) Earth-Venus-Mercury
2) Earth-Venus-Jupiter
3) Earth-Mars-Jupiter
4) Earth-Jupiter-Saturn
5) Earth-Jupiter-Outer planets
6) Earth-Jupiter-Sun

and (3) based on the results indicate which of these mission types warrant a detailed analysis.

The ground rules established for this study are as follows:

1) A two-dimensional solar system with circular ecliptic orbits for all planets except Mercury, which is assumed to have a coplanar orbit but with an eccentricity of 0.2,
2) A conic trajectory analysis, i.e., utilization of two-body equations of motion,
3) No launch or intercept time constraints - heliocentric trajectories are terminated when they reach the orbit radius of the gravity assist or the target body,
4) All trajectories begin from Earth's orbit,
5) Gravity assisted perturbations apply only to the velocity vector at the time the trajectory reaches a point mass which represents the gravity assist body,
6) Only one gravity assist maneuver between the Earth and the target objective.

Table 1 contains a consistent set of planetary data used for ASC/IITRI numerical trajectory analysis. The semi-major axes of the planets' orbits (except Mercury) were selected from the table as the circular orbit radii.

2. DISCUSSION OF METHOD

There are a number of methods for analyzing the gravity assist phase of an interplanetary trajectory. The technique selected in this study is, mathematically, perhaps the simplest.

TABLE I

PLANET DATA

Planet	Gravitational Parameter * K (km^3/sec^2)	Equatorial Radius R_o (km)	Semi-Major Axis of Orbit (AU)	Eccentricity of Orbit	Perihelion Distance (AU)	Aphelion Distance (AU)	Inclination of Orbit to Ecliptic	Mean Orbital Velocity Earth = 1	Period of Revolution (years)	Density Water = 1	Mass ☉ = 1	Period of Rotation h. m.
Mercury	2.168553×10^4	2,500	0.387099	0.2056259	0.307501	0.466697	7 0 14.2	1.607271	0.2411	5.00	0.0543	
Venus	3.247695×10^5	6,200	0.723332	0.0067935	0.718418	0.728246	3 23 39.1	1.175794	0.6156	4.90	0.8136	
Earth	3.986032×10^5	6,378	1.000000	0.0167272	0.983273	1.016727		1.0	1.0	5.52	1.0	23 56.068
Mars	4.297780×10^4	3,310	1.523691	0.0933654	1.381431	1.665951	1 50 50.8	0.8068546	1.8822	4.20	0.1077	24 37.38
Jupiter	1.267106×10^8	69,880	5.202803	0.0484305	4.950829	5.454777	1 18 19.9	0.4384109	11.86	1.33	318.35	9 50.5
Saturn	3.791870×10^7	57,550	9.538843	0.0556922	9.007604	10.070082	2 29 42.2	0.3237816	29.46	0.71	95.3	10 2
Uranus	5.803292×10^6	25,500	19.181973	0.0472012	18.276561	20.087385	0 46 22.9	0.2283249	84.0	1.26	14.58	10 48
Neptune	7.026072×10^6	25,000	30.057707	0.0085724	29.800040	30.315374	1 46 26.5	0.1823988	164.8	1.61	17.26	15 48
Pluto	3.317886×10^5	7,000 **	39.51774	0.2486438	29.691899	49.343581	17 8 38.4	0.7590757	247.7		0.8312	

* V. C. Clarke, Jr. (1962)

** Explanatory Supplement (1961)

All other data from Krafft A. Ehricke, (1960)

Earth's Mean Orbital Velocity = 29.77 km/sec

Earth Mass = 5.98×10^{27} g

It employs the concept of a sphere-of-influence as a geometrical definition of the gravitational field of the perturbing planet. The radius of the sphere has been defined by Laplace (Hohmann 1925) as

$$r_s = R_b \left(\frac{m_b}{M}\right)^{2/5} , \qquad (1)$$

where

R_b = the distance of the perturbing planet from the Sun,

m_b = the mass of the perturbing planet,

M = the mass of the Sun.

Table 2 (Stearns 1963) lists the radii of influence of the planets of the solar system. Since this study is restricted to a two-dimensional analysis, the region of activity will be referred to below as the circle-of-influence, COI.

The method is described by beginning with the hyperbolic escape velocity, VHL, and the injection flight path angle, γ, specified as initial conditions at escape from Earth (P_1). The heliocentric trajectory to the gravity assist planet (P_2) is determined as shown in Figure 1. The point of intersection of P_2's orbit becomes the fixed position of a point mass which represents the perturbing planet. While it is understood that the spacecraft's trajectory does not actually intersect P_2, the planet's orbit is a convenient boundary point at which to terminate the pre-assist heliocentric trajectory. The spacecraft's position, R_2, and velocity vector, $\bar{V}_{12}$, are computed at this point.

Table 2

RADII OF SPHERES OF INFLUENCE

Planet	Astronomical Units*	Kilometers x 10^{-4}	r_s/r_{planet}
Mercury	0.000746	11.16	46
Venus	0.00412	61.63	102
Earth	0.00618	92.45	142
Mars	0.00378	56.55	190
Jupiter	0.3216	4811.10	706
Saturn	0.3246	4855.98	848
Uranus	0.346	5176.13	2,180
Neptune	0.5805	8684.22	4,000
Pluto	0.2366	3539.51	$\sim$ 12,000

* 1 AU = 1.49599 x 10^8 kilometers

The distance traveled within the gravitational field of P_2 (COI) is small by comparison with the total trajectory distance from Earth (P_1) to the target planet (P_3). Therefore, it is assumed that a fixed position, equal to the position R_2 of the point mass of P_2, is sufficiently representative (on a heliocentric scale) of the spacecraft while it is within the COI. It is also assumed that the spacecraft's heliocentric velocity upon entering the COI at E may be approximated by the velocity vector, $\overline{V}_{12}$, as is shown in Figure 2.

The point of entrance, E, on the COI, with respect to P_2 is fixed by specifying the miss distance of closest approach, p, and knowing the heliocentric velocity vector, $\overline{V}_{12}$. Changes in E with new values of the parameter, p, are accommodated by small changes in the time of launch at Earth. The velocity, $\overline{V}_{21}$, with respect to P_2, at point E, as shown in Figure 2, is determined by the vector subtraction

$$\overline{V}_{21} = \overline{V}_{12} - \overline{V}_p \ , \qquad (2)$$

where $\overline{V}_p$ is the gravity assist planet's velocity vector at the position of its point mass. From the conservation of energy of the hyperbolic fly-by trajectory it can be shown that the velocity vector, $\overline{V}_{22}$, at the point of departure, L, of the COI is equal in <u>magnitude</u> to $\overline{V}_{21}$. However, the directions of $\overline{V}_{21}$ and $\overline{V}_{22}$ differ by an angle, α, as illustrated in Figure 2. The solution for the angle, α, is given as

$$\alpha = 2 \tan^{-1}\left(\frac{K_b}{V_{21}^2 B}\right), \qquad \text{(B9)}^*$$

where, B, the asymptotic miss distance is defined as

$$B = p_2\left(1 + \frac{2K_b}{p\, V_{21}^2}\right), \qquad \text{(B14)}$$

and

p = miss distance of closest approach,

V_{21} = asymptotic approach speed,

K_b = gravitational parameter of P_2.

The derivation of equations (B9) and (B14) is presented in Appendix B. Knowing the value of α and the velocity vector, $\overline{V}_{21}$, completely defines the vector, $\overline{V}_{22}$. Using simple vector addition, i.e.

$$\overline{V}_{31} = \overline{V}_{22} + \overline{V}_p , \qquad (3)$$

the post-assist heliocentric velocity vector, $\overline{V}_{31}$, illustrated in Figures 1 and 2, is determined.

Again neglecting small differences in position and velocity, the post-assist heliocentric trajectory is started at the point of P_2 with an initial heliocentric velocity vector equal to $\overline{V}_{31}$. The elements of the trajectory to P_3 are determined. The flight is terminated at the intersection of the orbit of P_3. The method is completed with the determination of the boundary conditions, i.e., position, velocity and time,

* Letters preceding equation numbers indicate that these equations have been derived in the Appendix bearing the same letter.

at the target. This method of analysis is, of course, an approximation of the true motion of a spacecraft on a gravity assisted mission.

The first mission discussed in the results is the Earth-Venus-Mercury flight. This case was selected to check the accuracy of the method by comparing the results with a similar case conducted by Minovitch (1963). He in turn has checked his data with exact solutions of the same mission (Cutting and Sturms 1964).

3. ANALYTICAL MAXIMUM FORMULAS

In addition to the above equations, there are analytical expressions* for the maximum velocity and energy changes which can be made by a gravity assisting body. The derivations of these expressions are given in Appendix C. The results and discussion are presented here.

Consider first the velocity change, DV, due to gravity assist. The maximum velocity change (from Appendix B) is

$$DV_{max} = V_h = \sqrt{\frac{K_b}{p}} \quad , \tag{C10}$$

where

V_h = hyperbolic approach velocity, V_{21} or V_{22}.

Several important conclusions may be drawn from equation (C10). First, the magnitude of the maximum velocity change is inversely proportional to the distance of closest approach, p. In other

* These analytical expressions were derived under the assumption of a 2-D solar system and two-body motion.

words, the closest approach possible (one body radius if no atmosphere exists) should be selected to afford the greatest change in the velocity vector. Secondly, only one constraint must be met by the pre-assist heliocentric trajectory for maximum velocity change. It is given by the relation

$$\left| \overline{V}_{12} - \overline{V}_p \right| = V_{21} = \sqrt{\frac{K_b}{p}} \ . \qquad (4)$$

For a given value of p, a great number of $\overline{V}_{12}$ vectors satisfy equation (4). Hence there are many pre-assist heliocentric trajectories which provide a maximum DV maneuver at the gravity assist body. Some of these trajectories could be achieved with an Earth launch.

The maximum energy change, ΔE, due to a gravity assist is

$$\Delta E_{max} = V_p \, V_h = V_p \sqrt{\frac{K_b}{p}} \ , \qquad (C19)$$

with the constraint that

1) $\beta_1 = 120°$ and $\beta_2 = 60°$ for energy addition,

2) $\beta_1 = 60°$ and $\beta_2 = 120°$ for energy subtraction.

The angles β_1 and β_2 are defined in Figure 2. The case of maximum energy addition is illustrated in the figure.

The condition for maximum velocity change given in equation (C10) is

$$V_h = \sqrt{\frac{K_b}{p}} \ . \qquad (C10)$$

Examining eq. (C19) above, it is obviously concluded that the maximum

energy change case is also a maximum velocity change case. However, the conditions for maximum energy change are more restrictive than those that apply to maximum velocity change. The velocity vector, $\overline{V}_{12}$, at point E in Figure 2 is completely defined by the following constraints for maximum energy change:

1) $V_{21} = \sqrt{\frac{K_b}{p}}$,

2) $\beta_1 = 120°$ (for maximum energy addition),

3) $\overline{V}_p$ = velocity vector of the gravity assist body.

The same reasoning is applicable to the definition of the velocity vector, $\overline{V}_{31}$, at point L in Figure 2. Since the heliocentric position of the spacecraft during its traversal of the COI is assumed fixed (and equal to the gravity assist body's solar position which defines the third constraint above, $\overline{V}_p$) the heliocentric pre-assist and post-assist trajectories associated with maximum energy change are unique and known. From the symmetry of the energy addition and subtraction solutions it can also be shown that these trajectories are just reversed (post-assist becoming pre-assist and vice versa) when maximum energy subtraction rather than addition is considered. From the calculation of the perihelion and aphelion of these trajectories it is possible to determine whether or not a maximum energy transfer at the specified gravity assist body can be achieved with a launch from Earth.

Table 3 contains a list of the planets of the solar system, ordered according to the maximum DV available for a miss distance of one planet radius. A second list is given but ordered according to the maximum ΔE available. Included in Table 3 are the perihelion and aphelion of the required heliocentric trajectories to affect the maximum energy change. Notice that the ordering of planets differs between the two lists. This is explained by the fact that the maximum energy change (equation (C19)) is a function of the planet velocity, V_p, as well as the gravitational parameter, K_b, and the distance of closest approach, p. Only K_b and p are required to determine the maximum velocity change (equation (C10)).

4. NUMERICAL APPROACH

A numerical program for the IBM 7094 Digital Computer was constructed to investigate gravity assisted missions in the manner discussed above. The program was formulated on the ground rules given in the introduction and does not recognize the launch-intercept date problem, i.e., it does not generate launch opportunities. Therefore the results of the mission studies below can only be considered as parametric conclusions and do not in general apply to any given launch period. A notable exception to this restriction is the Earth-Jupiter-Solar Probe mission.

In addition to the ground rules set forth in the introduction the following definitions were used for the numerical approach:

Table 3

ORDERED LISTS OF MAXIMUM VELOCITY AND ENERGY CHANGES
DUE TO PLANETARY GRAVITY ASSIST

3A - Velocity Change

	Planet	Maximum Velocity Change, km/sec
1.	Jupiter	42.6
2.	Saturn	25.7
3.	Neptune	16.8
4.	Uranus	15.1
5.	Earth	7.9
6.	Venus	7.2
7.	Pluto	6.9
8.	Mars	3.6
9.	Mercury	3.0

3B - Energy Change

	Planet	Maximum Energy Addition, km^2/sec^2	Perihelion Before, AU	Aphelion Before, AU	Perihelion After, AU	Aphelion After, AU
1.	Jupiter	583.7	0.59	Hyperbolic	3.30	Hyperbolic
2.	Saturn	261.7	0.31	Hyperbolic	6.22	Hyperbolic
3.	Venus	255.2	0.47	0.77	0.68	1.25
4.	Earth	239.4	0.58	1.09	0.92	2.12
5.	Mercury	173.7	0.31	0.42	0.31	0.53
6.	Uranus	107.6	0.03	Hyperbolic	13.00	Hyperbolic
7.	Mars	95.5	1.16	1.51	1.34	2.40
8.	Neptune	91.9	3.26	Hyperbolic	19.86	Hyperbolic
9.	Pluto	42.1	3.66	100.09	23.85	Hyperbolic

1) Ideal velocity is defined as

$$\Delta V = \sqrt{(VHL)^2 + (36{,}178)^2} + 4000 \text{ ft/sec.}$$

2) Total trip time is defined as the sum of the trip times of heliocentric trajectories between Earth and the gravity assist body and between the gravity assist body and the target body.

The program performs an automatic parametric variation of the hyperbolic excess velocity, VHL, the initial injection flight path angle, γ, (see Figure 1) and the distance of closest approach at the gravity assist planet, p. The resulting trip time is plotted against these parameters. Trajectory performance conclusions for the mission under consideration are drawn from these and associated cross plots. The graphs will be discussed briefly below before the mission performance results are presented. The program requires only about 0.1 seconds on the IBM 7094 to generate a complete trajectory from launch to target.

5. MISSION RESULTS

In Table 3 it can be seen that Jupiter provides both the maximum velocity change and the maximum energy change. The variation of the velocity and energy changes with miss distance at Jupiter is plotted in Figure 3. The figure illustrates that the gains in velocity and energy changes increase rapidly as the miss distance approaches the radius of Jupiter. Improvements in trajectory performance gained through gravity assist, are conveniently measured by the velocity change

achieved. Therefore, where mission constraints allow, it is usually most advantageous to pass as close to the gravity assist planet as is possible.

Factors which constrain the performance of gravity assisted trajectories are 1) planetary atmospheres, 2) accuracy of tracking, 3) plane changes required in three-dimensional space, and 4) phasing requirements imposed by the physical positions of the planets at the time of launch. The first two items, in particular, prohibit the use of a grazing approach to the perturbing planet. Nevertheless, in preparing the numerical data, it was decided that the best gains in performance from gravity assist should be presented despite these physical limitations. Therefore, the results of this study represent a reference upper limit in the advantage of ballistic gravity assisted trajectories over direct flights. Sufficient additional data has been included to assess performance degradation due to other than grazing miss distances at the gravity assisting planet.

5.1 Earth-Venus-Mercury

The trajectory for this mission begins at Earth (P_1), flys by Venus (P_2) and intercepts Mercury (P_3). Due to the ellipticity of Mercury's orbit, two intercept cases were studied; 1) Mercury at its perihelion, and 2) Mercury at its aphelion.

Figure 4 is the "data" graph from which the mission analysis is made; it is plotted directly from computer output.

The total trip time from P_1 via P_2 to P_3 is given on the ordinate and the distance of closest approach to P_2 is given in body radii along the abscissa. Each curve on the graph is plotted for a different ideal velocity. A miss distance of one corresponds to skimming the surface of P_2. The surface radius of P_2 is given in kilometers along the vertical dotted line. It should be noted that every point on the graph represents a specific gravity assisted trajectory with a defined ideal velocity, trip time and miss distance.

Figures 4 and 5 are plotted for Mercury at its perihelion (0.31 AU). Observe in Figure 4, for a fixed miss distance, that the improvement (decrease) in trip time is reduced at the higher ideal velocities. For a fixed ideal velocity the shortest trip time (indicated by a circle on each velocity curve) occurs with the closest possible approach to Venus, i.e., 6200 kilometers. These minimum trip time points may be replotted as a function of ideal velocity and time to construct a "minimum time" mission curve. This is done in Figure 5. For comparison, a direct mission curve from P_1 to P_3 is also plotted against ideal velocity and trip time. The gravity assisted flights are better than the direct flights when the ideal velocity is less than 52,200 ft/sec. That is, fixing either ideal velocity or trip time reduces the other with the gravity assist technique.

As an example of the energy savings, the minimum ideal velocity required for a direct trip to Mercury (at perihelion) is 51,400 ft/sec requiring 96 days to get there. For the same trip time the Venus fly-by mission to Mercury requires an ideal velocity of 48,700 ft/sec, i.e., a reduction of 2700 ft/sec. Selecting a 120 day trip time and using a Venus assist, the required velocity to reach Mercury is further reduced to 45,000 ft/sec.

The "data" graph for Mercury at its aphelion (0.47 AU) is shown in Figure 6. Again the best trip time at a fixed ideal velocity is achieved at the smallest miss distance of Venus, but note now that the initial ideal velocity required to reach Mercury is much less than in Figure 4, i.e., 41,500 ft/sec instead of 45,200 ft/sec. The "minimum time" mission curve is plotted in Figure 7. Here the break even point between direct and gravity assisted flights is at 46,250 ft/sec and 95 days trip time. At higher velocities direct flights are better and below this gravity assisted flights are better. Although the gravity assist savings are not as significant when Mercury is at its aphelion, the ideal velocity requirements are so low for the Venus fly-by missions with trip times greater than 140 days as to make medium class launch vehicles attractive. With the gravity assist from Venus, Mercury can be reached in 170 days with an ideal velocity of 41,500 ft/sec. For this mission the Atlas-Agena launch vehicle has a payload capability of 580 pounds; the Atlas-Centaur provides a payload of 1900 pounds.

As a check of the two-dimensional analysis, the variation of ideal velocity and trip time across an actual launch window

(7/25/70 to 9/13/70) of an Earth-Venus-Mercury (0.47 AU) mission was added to Figure 7. The data for this launch window curve was taken from a complete three-dimensional analysis of this particular mission (Minovitch 1963). The curve represents the best launch window between 1965 and 1973. There is less than one percent difference in ideal velocity between the two curves at their closest point. Part of the difference between the "minimum time" curve and the launch window curve is explained by geometry constraints which dictated miss distances somewhat greater than the optimum for an actual opportunity. A two-dimensional example for this launch window is illustrated in Figure 8*.

Several observations can be made in summarizing the missions to Mercury. If very short flight times are required at the cost of higher ideal velocities, direct missions are superior. Gravity assist missions to Mercury are definitely desirable with longer trip times, or smaller launch vehicles. In fact if the trip time is relaxed beyond 120 days, these missions impose only modest launch vehicle requirements. Venus objectives should not be too difficult to accomplish during fly-by. The VHP for gravity assist is only about 10% higher than the hyperbolic approach speed of a direct Venus fly-by mission. Guidance requirements for a gravity assist flight, while usually more stringent than they are for direct flight, have been shown to be modest (Cutting and Sturms 1964). For the 1970 Venus fly-by to Mercury 150 pounds of propellant and propulsion hardware are required of a 1300 pound spacecraft for midcourse corrections. Even though this is more

* A similar example has been illustrated by Minovitch.

than would be required for a direct flight to Mercury, its effect on spacecraft weight is small when compared to the payload growth realized by the reduction in ideal velocity for gravity assisted flights.

5.2 Earth-Venus-Jupiter

A study of the Earth-Venus-Jupiter mission revealed that this combination of planets for a gravity assisted flight to Jupiter is very inefficient. Over the range of ideal velocities between 48,000 and 54,000 ft/sec, for Venus miss distances from one to ten Venus radii, and all angles of γ (0° to -180°; see Figure 1), the furthest point reached by all post-Venus trajectories was less than 3 AU from the Sun. This is contrasted by an aphelion of greater than 10 AU for a direct, Earth departure trajectory (perihelion of 1 AU) with an ideal velocity of 54,000 ft/sec. After all the results were tabulated, it was concluded that the Earth-Venus-Jupiter flight was the least favorable gravity assisted mission considered in the study.

5.3 Earth-Mars-Jupiter

The "data" graph for the Earth-Mars-Jupiter flight is plotted in Figure 9. The shortest time points are replotted to form the "minimum time" mission curve in Figure 10. Compared to the direct flight curve it shows little improvement in either ideal velocity or flight time except at the lower end of the curve ($\Delta V < 51{,}000$ ft/sec).

A cursory look at launch opportunities revealed that the next Earth-Mars-Jupiter launch period occurs in 1984. A particular flight for this opportunity is shown in Figure 11

along with some time varying distance curves in Figure 12. It is observed that the Mars gravitational field does not affect a significant variation in that trajectory. This restriction coupled with the long Earth-Mars synodic period (780 days) accounts for the rarity of launch opportunities. It may be possible, however, with a more detailed three-dimensional analysis to determine one or two additional launch opportunities to Jupiter via Mars before 1984. In addition to the opportunity shortage the approach velocity to Mars is more than twice as large as a direct Mars fly-by mission, e.g. 14.9 km/sec for the case illustrated in Figure 12. Hence it becomes difficult to accomplish Mars objectives during fly-by. Considering the added complexity in the mission profile of the Jupiter mission when a Mars assist is included, and the moderate returns in trajectory performance, as with Venus there is reason to favor the direct rather than gravity assisted flights to Jupiter.

5.4 Earth-Jupiter-Saturn

The "data" graph for Earth-Jupiter-Saturn missions is plotted in Figure 13. Unlike Venus and Mars assists, the minimum time points on the ideal velocity curves do not occur at the closest possible approach to Jupiter. The explanation for this is both gravitational and geometrical.

It has been shown in Figure 3 that the closer the spacecraft comes to Jupiter for a gravity assist the more velocity transfer that results. For Earth launched flights a near Jupiter miss is reflected in the post-assist heliocentric

trajectory by giving the spacecraft a more tangential departure to Jupiter's orbit. Figure 14 illustrates this effect. With a very large miss distance (no effective velocity change) the spacecraft proceeds along its pre-assist trajectory to P_3 at point B. But, with a near miss at P_2 (large velocity addition) the flight path is bent toward the orbit of P_2 and consequently the spacecraft intercepts P_3 at point C.

Now, when P_3's orbit radius does not differ greatly from that of P_2, i.e., R_3 is less than $2R_2$, the radial distance (AB in Figure 14) between orbits is significantly smaller than the distance (AC) along a line which is tangential to P_2's orbit. Therefore, a trade-off in trip time exists between the faster but longer route to P_3 at point C as a result of a near miss at P_2 and the shorter but slower route to P_3 at point B due to a large miss at P_2. The trade-off results in shortest time trajectories to Saturn having miss distances at Jupiter of several radii as shown in Figure 13. However, when the radius of P_3 becomes much larger than R_2 the difference between the tangential and radial distances to R_3 diminishes and the shortest time points fall back to a skimming approach of P_2. For Jupiter this phenomenon is observed in Figures 17 and 19 where the target radius is increased to 20 AU and 50 AU respectively.

The numerical data for this mission also indicates that a minimum energy trajectory to Jupiter (ΔV = 51,200 ft/sec) gains enough energy through gravity assist to extend the post-assist

heliocentric trajectory out a great deal further (about 370 AU) than Jupiter's orbit. This means that a Hohmann transfer to Jupiter is sufficient to accomplish a Saturn mission if Jupiter's gravity field is properly utilized. The "minimum time" mission curve for a Jupiter fly-by to Saturn is plotted along with the direct curve in Figure 15. Notice here that not only do the time savings become significant for gravity assist as ideal velocity is reduced below 55,000 ft/sec, but at a given time, e.g. 3.5 years, the ideal velocity requirement is reduced enough from direct flight (from 55,000 to 52,000 ft/sec) to allow significant payloads to be sent to Saturn with existing launch vehicles, i.e., the Saturn booster family.

A particular Earth-Jupiter-Saturn mission, along with some specific trajectory data, is illustrated in Figure 16 for a 1977 launch opportunity. Opportunities for similar missions also occur (based again on a 2-D study) in 1976 and 1978. The figure is self-explanatory, but it is worth noting that the equivalent DV at Jupiter due to gravity assist is 18.7 km/sec. For the same miss distance, 4 Jupiter radii, Figure 3 indicates the maximum available equivalent DV is 21 km/sec. This shows good utilization of Jupiter's gravitational field for velocity transfer by the illustrated mission in Figure 16.

The launch dates are frequent, when they occur, and they occur far enough in the future to plan an investigation program for the planet Saturn. The velocity requirements are low enough to allow payloads greater than 1000 pounds to be

launched with a Saturn 1B-Centaur class launch vehicle. The trip time is on the order of three years. This appears to be one of the better gravity assist missions and certainly warrants further, more detailed study.

5.5 Earth-Jupiter-Outer Planets

Figures 17 through 20 characterize missions via Jupiter to the outer planets by considering two target radii of 20 AU and 50 AU, rather than any specific planetary orbits. The advantages of gravity assist over direct flights to these distances are similar to those of the Earth-Jupiter-Saturn mission, only magnified. For the 20 AU mission (Fig. 18), beginning with an ideal velocity of 56,000 ft/sec, the Jupiter fly-by reduces the trip time from 13 to 5 years. In Figure 20, with an ideal velocity of 56,000 ft/sec, the trip time with a Jupiter assist is 11.5 years. A direct flight launched at Earth with this same ideal velocity will not reach 50 AU.

Preliminary comparisons of direct thrusted trajectories and direct ballistic trajectories have also shown significant improvements in performance for similar targets, but in favor of a thrusted propulsion system. It is, therefore, quite reasonable to expect a gravity assisted, thrusted approach to the exploration of the outer solar system to be even more desirable than either of these simpler schemes. In addition, the thrusted propulsion system can double as midcourse guidance control, which is usually more demanding with a gravity assist maneuver. It remains, of course, to analyze the feasibility

of such a hybrid trajectory.

5.6 Earth-Jupiter-Solar Probe

The last mission considered in the study was a solar probe via Jupiter. Figure 21 is a graph of total trip time versus ideal velocity for these missions. Lines of constant perihelion (after the gravity assist) and lines of constant miss distance at Jupiter are shown on the plot. From the figure, for an ideal velocity of 52,500 ft/sec and a miss distance of six Jupiter radii, there exists a trajectory which comes within 0.3 AU of the center of the Sun 3.15 years after leaving Earth. Each point within the grid represents a valid solar probe trajectory via a Jupiter fly-by. As a second example consider an ideal velocity of 54,000 ft/sec and a trip time of approximately three years. The closest approach to the Sun is 0.02 AU and the required miss distance at Jupiter is 5.3 Jupiter radii. The trajectory for this example is illustrated in Figure 22.

Note that about 400 days of the trip is spent in the asteroid belt. This places the spacecraft in a potentially hazardous environment for a long time. On the other hand, asteroid belt experiments could be conducted during the flight as a secondary objective of the mission. Another secondary objective for a Jupiter assisted solar probe would be the examination of Jupiter during fly-by. Present studies (Witting 1965) indicate that instruments designed to measure

particles and fields around Jupiter and around the Sun are similar, with regards to both type and sensitivity.

The maximum communication distance for the illustrated mission has been minimized by selecting a trajectory which permits the spacecraft to arrive at Jupiter just as the Earth comes between Jupiter and the Sun. A complete time history of communication distance and the distance between the spacecraft and the Sun is plotted in Figure 23.

The launch opportunities for this mission are frequent and consistent. Normally, when a gravity assisted trajectory involving three bodies (P_1, P_2, and P_3) is analyzed, the time between opportunities can be long or the elements of the required trajectory can change significantly from one opportunity to the next. Here this is not true. The opportunities present themselves once about every 13 months and show only minor changes in trajectory requirements. Hence there is little time restriction to the utilization of Jupiter for a solar fly-by mission.

The final Figure 24 shows a comparison of different modes of approaching the Sun from Earth. Plotted against ideal velocity and final perihelion are curves for direct, Venus fly-by and constant time Jupiter assisted trajectories. For the Venus fly-by and the direct curves the trip time is not constant. Several trip times have been pinpointed on these curves to show magnitude and variation of time. To reach the apparent edge (0.005 AU) of the Sun directly requires almost

100,000 ft/sec. A Venus fly-by requires about 95,000 ft/sec. To reduce the perihelion below 0.1 AU a Jupiter fly-by should be used. The trip time is a definite penalty but the energy requirements are much more reasonable. Another possibility for sending a spacecraft close to the Sun would be, of course, the use of a thrusted upper stage vehicle. The Jupiter assisted solar probe is an attractive multiple mission with frequent (approximately one per year) launch opportunities; it should receive a more thorough analysis.

6. CONCLUSIONS

The results of the study have already been helpful in the planning of long range programs. The analysis method used provides a simple selection process of those missions which are worthy of further investigation. For the interesting missions, the problems of

1) determining accurate launch opportunities,
2) analyzing guidance requirements, and
3) three dimensions

need more detailed study and analysis.

A study of these problems requires a comprehensive three-dimensional gravity assist and guidance computer program. In addition to providing increased accuracy for favorable gravity assisted missions, this code could be used to look at out-of-ecliptic missions in detail and enable gravity assist accessible regions (Narin 1964) contours to be generated.

Finally there is the possibility of gravity assisted thrusted missions. At some time in the future an effort should be made to determine the feasibility and performance gains of this hybrid trajectory scheme.

REFERENCES

Clarke, Jr., V. C., "Constants and Related Data Used in Trajectory Calculations at the Jet Propulsion Laboratory", JPL TR No. 32-273, 1962, p. 11.

Cutting, E. and Sturms, F. M., Jr., "Trajectory Analysis of a 1970 Mission to Mercury via a Close Encounter with Venus", JPL TM No. 312-505, December 7, 1964.

Dobson, Wilbur F., Huff, Vearl N., and Zimmerman, Arthur V., "Elements and Parameters of the Osculation Orbit", NASA TN D-1106, January 1962.

Ehricke, K. A., Space Flight-1. Environment and Celestial Mechanics, D. Van Nostrand, 1960.

Hohmann, W., Die Erreichbarkeit der Himmilskorper, R. Ouldenbourg, Munich, 1925.

Hunter, II, Maxwell W., "Future Unmanned Exploration of the Solar System", Astronautics and Aeronautics, May 1964, p. 16.

Minovitch, Michael A., "The Determination and Characteristics of Ballistic Interplanetary Trajectories Under the Influence of Multiple Planetary Attractions", JPL TR No. 32-468, October 31, 1963.

Narin, F., "The Accessible Regions Method of Energy and Flight Time Analysis for One-Way Ballistic Interplanetary Missions", ASC/IITRI Report No. T-6, 1964.

Stearns, Edward V. B., Navigation and Guidance in Space, Prentice-Hall Inc., N. J., 1963, p. 198.

Witting, James M., private communications, 1965.

1.1 Earth radii, from Explanatory Supplement to the Astronomical Ephemeris and the American Ephemeris and Nautical Almanac, H. M. Nautical Office, 1961, p. 491.

Appendix A

NOMENCLATURE

AU	Astronomical unit, 1 AU = 1.496×10^8 km
a	Semi-major axis, negative for a hyperbola
B	Asymptotic miss distance (see Figure 2)
COI	Two-dimensional circle of planetary influence
ΔV	Ideal velocity given to the spacecraft on leaving Earth: $\Delta V = \sqrt{(VHL)^2 + (36,178)^2} + 4000$ ft/sec. Here 36,178 ft/sec is the characteristic velocity for Earth escape launching from Cape Kennedy and 4000 ft/sec is a correction for gravitational and friction losses during launch.
DV	Equivalent velocity increment given to the spacecraft by a gravity assist, km/sec.
ΔE	Equivalent change in energy given to the spacecraft by a gravity assist, km^2/sec^2.
K_b	Gravitational parameter for the gravity assist body.
M	Mass of the Sun
m_b	Mass of the disturbing body
P_1	Earth, the planet from which all trajectories are initiated
P_2	Gravity assist planet

P_3	Target-intercept planet
p	Distance of closest approach, planet radii
R_b	Distance of the disturbing body from the Sun
R_1	Orbit radius of Earth
R_2	Orbit radius of the gravity assist planet
R_3	Orbit radius of the target-intercept planet
r_s	Radius of the sphere-of-influence and COI
VHL	Launch hyperbolic excess speed, that is, the difference between the spacecraft heliocentric velocity and Earth's velocity in its orbit, at the time when the spacecraft leaves the Earth.
VHP	Hyperbolic excess speed at planet intercept
V_h	Hyperbolic excess speed at the COI with respect to P_2
V_p	Planetary orbital speed
V_{12}	Heliocentric velocity at intercept of P_2
V_{21}	Hyperbolic approach velocity, V_h, with respect to P_2
V_{22}	Hyperbolic departure velocity, V_h, with respect to P_2
V_{31}	Heliocentric velocity at departure of P_2
α	Angle between approach and departure asymptotes at P_2 (see Figure 2)
β_1	Angle between $\overline{V}_p$ and $\overline{V}_{21}$
β_2	Angle between $\overline{V}_p$ and $\overline{V}_{22}$
γ	Injection flight path angle (see Figure 1)
ϕ	See Figure 2
Ψ	See Figure 2

Appendix B

DERIVATION OF GRAVITY ASSIST EQUATIONS

It has been shown in Section 2 and Figure 2 that the approach velocity vector, $\overline{V}_{21}$, and the departure velocity vector, $\overline{V}_{22}$, of a gravity assist maneuver are equal in magnitude but not direction. The vector $\overline{V}_{21}$ lies along the approach asymptote and the vector $\overline{V}_{22}$ lies along the departure asymptote. These asymptotes of the hyperbolic fly-by trajectory differ by an angle, α.

The angle α is written as the function

$$\alpha = f\ (B,\ V_{21},\ K_b)\ , \qquad \text{(B1)}$$

where,

B = asymptotic miss distance,

V_{21} = asymptotic approach velocity,

K_b = gravitational parameter of the gravity assist planet.

To determine the function of equation (B1) note from Figure 2 that

$$\alpha = \pi - 2\,\phi\ , \tag{B2}$$

$$\Psi = \frac{\pi}{2} - \phi\ . \tag{B3}$$

Combining equations (B2) and (B3),

$$\alpha = \pi - 2\left(\frac{\pi}{2} - \Psi\right),$$

$$\alpha = 2\Psi\ . \tag{B4}$$

Also from Figure 2,

$$\tan\Psi = \frac{|a|}{B}\ . \tag{B5}$$

Using the energy equation* for a hyperbola,

$$E = \frac{V^2}{2} - \frac{K}{R} = -\frac{K}{2a}\ . \tag{B6}$$

Since V_{21} is defined as the asymptotic approach velocity, it may be considered as the spacecraft velocity (with respect to P_2) at an infinite distance from the gravity assist planet. Hence, substituting V_{21} into equation (B6) yields

$$\frac{V_{12}^{\ 2}}{2} = -\frac{K_b}{2a}\ ,$$

or

$$|a| = \frac{K_b}{V_{21}^{\ 2}}\ . \tag{B7}$$

Substituting (B7) into (B5),

---

* A complete table of two-body equations of motion has been formulated by Dobson, Huff and Zimmerman (1962).

$$\Psi = \tan^{-1}\left(\frac{K_b}{V_{21}^2\, B}\right), \tag{B8}$$

and combining (B8) with (B4) the solution to equation (B1) is given as

$$\alpha = 2\,\tan^{-1}\left(\frac{K_b}{V_{21}^2\, B}\right). \tag{B9}$$

The asymptotic miss distance, B, can be expressed as the function

$$B = f\,(V_{21},\, K_b,\, p)\ , \tag{B10}$$

where V_{21} and K_b are the same as before, and

p = distance of closest approach to P_2.

To solve the function of (B10) note from ΔACD in Figure 2 that

$$c^2 = a^2 + b^2\ . \tag{B11}$$

Since ΔOPD is similar to ΔACD equation (B11) becomes

$$(p + a)^2 = a^2 + B^2\ . \tag{B12}$$

Expanding, and making the proper cancellations,

$$p^2 + 2ap + a^2 = a^2 + B^2\ ,$$

$$B^2 = p^2\,(1 + \frac{2a}{p})\ . \tag{B13}$$

Substituting (B7) into (B13) yields the solution of the function in (B10), which is

$$B^2 = p^2\left(1 + \frac{2K_b}{p\ V_{21}^2}\right). \tag{B14}$$

Through the use of equation (B14) it was possible in the numerical analysis to use the distance of closest approach, p, as a parameter of variation rather than the asymptotic miss distance, B, which is used in equation (B9).

Appendix C

DERIVATION OF MAXIMUM FORMULAS

There exist analytical equations, consistent with the assumptions stated in the introduction, for maximum velocity and maximum energy changes from the gravity assist of a planet. Consider first the derivation for maximum velocity change.

The velocity change, DV, due to gravity assist is given by the vector equation

$$D\overline{V} = \overline{V}_{31} - \overline{V}_{12} \ , \tag{C1}$$

as can be seen from Figure 2. But,

$$\overline{V}_{12} = \overline{V}_{21} + \overline{V}_{p} \ ,$$

and

$$\overline{V}_{31} = \overline{V}_{22} + \overline{V}_{p} \ .$$

Substituting into equation (C1) yields,

$$D\overline{V} = \overline{V}_{22} - \overline{V}_{21} \ . \tag{C2}$$

Squaring equation (C2),

$$DV^2 = (\overline{V}_{22} - \overline{V}_{21}) \cdot (\overline{V}_{22} - \overline{V}_{21}) ,$$

$$= V_{21}^2 + V_{22}^2 - 2\overline{V}_{22} \cdot \overline{V}_{21} . \qquad (C3)$$

By definition,

$$V_h = V_{21} = V_{22} .$$

Hence equation (C3) becomes,

$$DV^2 = 2V_h^2 - 2V_h^2 \cos \alpha , \qquad (C4)$$

(see Figure 2 for the definition of α). Since

$$\alpha = 2\Psi , \qquad (B4)$$

equation (C4) becomes,

$$DV^2 = 2V_h^2 - 2V_h^2 (1 - 2 \sin^2 \Psi)$$

$$= 4V_h^2 \sin^2 \Psi .$$

So that by taking the square root the velocity change, DV, is,

$$DV = 2V_h \sin \Psi . \qquad (C5)$$

From Figure 2,

$$\sin \Psi = \frac{a}{a + p} . \qquad (C6)$$

Substituting equation (B7) into (C6),

$$\sin \Psi = \frac{K_b/V_h^2}{K_b/V_h^2 + p} = \frac{K_b}{pV_h^2 + K_b} , \qquad (C7)$$

and combining equations (C5) and (C7),

$$DV = \frac{2V_h K_b}{pV_h^2 + K_b} . \qquad (C8)$$

Now to maximize DV it is obvious that the miss distance, p, should be chosen as small as possible. With p specified (constant), the V_h which maximizes DV is found by differentiating equation (C8) with respect to V_h. Hence,

$$\frac{d\,(DV)}{dV_h} = \frac{2K_b}{pV_h^2 + K_b} - \frac{4K_b\, pV_h^2}{(pV_h^2 + K_b)^2} = 0 ,$$

$$0 = 2K_b\,(pV_h^2 + K_b) - 2K_b\, pV_h^2 ,$$

$$0 = 2K_b\, pV_n^2 - 2K_b^2 - 4K_b\, pV_h^2 .$$

Transposing,

$$2K_b\, pV_h^2 = 2K_b^2 ,$$

$$V_h = \sqrt{\frac{K_b}{p}} . \qquad (C9)$$

Substituting (C9) into (C8),

$$DV_{max} = \frac{2K_b\sqrt{K_b/p}}{pK_b/p + K_b} ,$$

$$= \sqrt{\frac{K_b}{p}} .$$

So that,

$$DV_{max} = V_h = \sqrt{\frac{K_b}{p}} \, . \tag{C10}$$

Consider now the case of maximum energy change. Since heliocentric position changes of the spacecraft were ignored during the gravity assist,

$$\left| \Delta E \right| = 1/2 \left| V_{31}^2 - V_{12}^2 \right| , \tag{C11}$$

or in vector notation

$$\left| \Delta E \right| = \left| \overline{V}_p \cdot (\overline{V}_{22} - \overline{V}_{21}) \right| , \tag{C12}$$

since from Figure 2,

$$V_{12}^2 = V_p^2 + V_{21}^2 + 2V_p V_{21} \cos \beta_1 ,$$

$$V_{31}^2 = V_p^2 + V_{22}^2 + 2V_p V_{22} \cos \beta_2 ,$$

$$V_{31}^2 - V_{12}^2 = 2V_p V_{22} \cos \beta_2 - 2V_p V_{21} \cos \beta_1 ,$$

$$= 2\overline{V}_p \cdot (\overline{V}_{22} - \overline{V}_{21}) \, .$$

To maximize equation (C12) for ΔE it is apparent that two conditions are to be satisfied. They are as follows:

1) $\left| \overline{V}_{22} - \overline{V}_{21} \right|$ should be maximized,

2) $\overline{V}_p$ and $(\overline{V}_{22} - \overline{V}_{21})$ should be colinear, i.e., the angle between $(\overline{V}_{22} - \overline{V}_{21})$ and $\overline{V}_p$ should be 0° for energy addition and 180° for energy subtraction.

For condition 1) note from equation (C2) that,

$$\left| \overline{V}_{22} - \overline{V}_{21} \right| = DV \ .$$

Hence the maximum value of $\left| \overline{V}_{22} - \overline{V}_{21} \right|$ is given by equation (C10) as,

$$\left| \overline{V}_{22} - \overline{V}_{21} \right|_{max} = V_h = \sqrt{\frac{K_b}{p}} \ . \qquad (C13)$$

The value of the angle α between $\overline{V}_{22}$ and $\overline{V}_{21}$ (see Figure 2 for definition) may be found from equations (C5) and (C10). Since from equation (C13) one condition for maximum energy change is that the velocity change be maximum, equation (C5) may be rewritten as

$$V_h = 2V_h \sin \Psi \ ,$$

or,

$$\sin \Psi = 1/2 \ ,$$

then,

$$\alpha = 2\Psi = 60° \ . \qquad (C14)$$

The condition of colinearity for maximum energy change is given in equation form as,

$$\left| \overline{V}_p \cdot (\overline{V}_{22} - \overline{V}_{21}) \right| = V_p \left| \overline{V}_{22} - \overline{V}_{21} \right| \ .$$

Expanding and using the results in equation (C13),

$$\left| V_p V_{22} \cos \beta_2 - V_p V_{21} \cos \beta_1 \right| = V_p V_h \ . \qquad (C15)$$

Hence, since $V_{21} = V_{22} = V_h$, equation (C15) becomes,

$$V_p V_h \left| \cos \beta_2 - \cos \beta_1 \right| = V_p V_h ,$$

or,

$$\left| \cos \beta_2 - \cos \beta_1 \right| = 1 . \qquad \text{(C16)}$$

The angles β_1 and β_2 are not independent. From Figure 2 it can be seen that their constraint equation is given by

$$\beta_1 - \beta_2 = \alpha . \qquad \text{(C17)}$$

Substituting equation (C14) into (C17),

$$\beta_1 - \beta_2 = 60° . \qquad \text{(C18)}$$

The conditions for maximum energy change are now set. Using equations (C12), (C15) and (C13) the equation of maximum energy is found to be,

$$\left| \Delta E \right|_{max} = V_p V_h = V_p \sqrt{\frac{K_b}{p}} . \qquad \text{(C19)}$$

From equations (C16) and (C18) the values of β_1 and β_2 for maximum energy <u>addition</u> are,

$$\beta_1 = 120° , \quad \beta_2 = 60° , \qquad \text{(C20)}$$

since the angle between $(\overline{V}_{22} - \overline{V}_{21})$ and $\overline{V}_p$ is 0° (this is the case illustrated in Figure 2). The values of β_1 and β_2 for maximum energy <u>subtraction</u> are,

$$\beta_1 = 60° , \quad \beta_2 = 120° , \qquad \text{(C21)}$$

since the angle between $(\overline{V}_{22} - \overline{V}_{21})$ and $\overline{V}_p$ is 180°.

FIGURES

The following figures have been assembled together for ease of reference. They are referred to by number throughout the report.

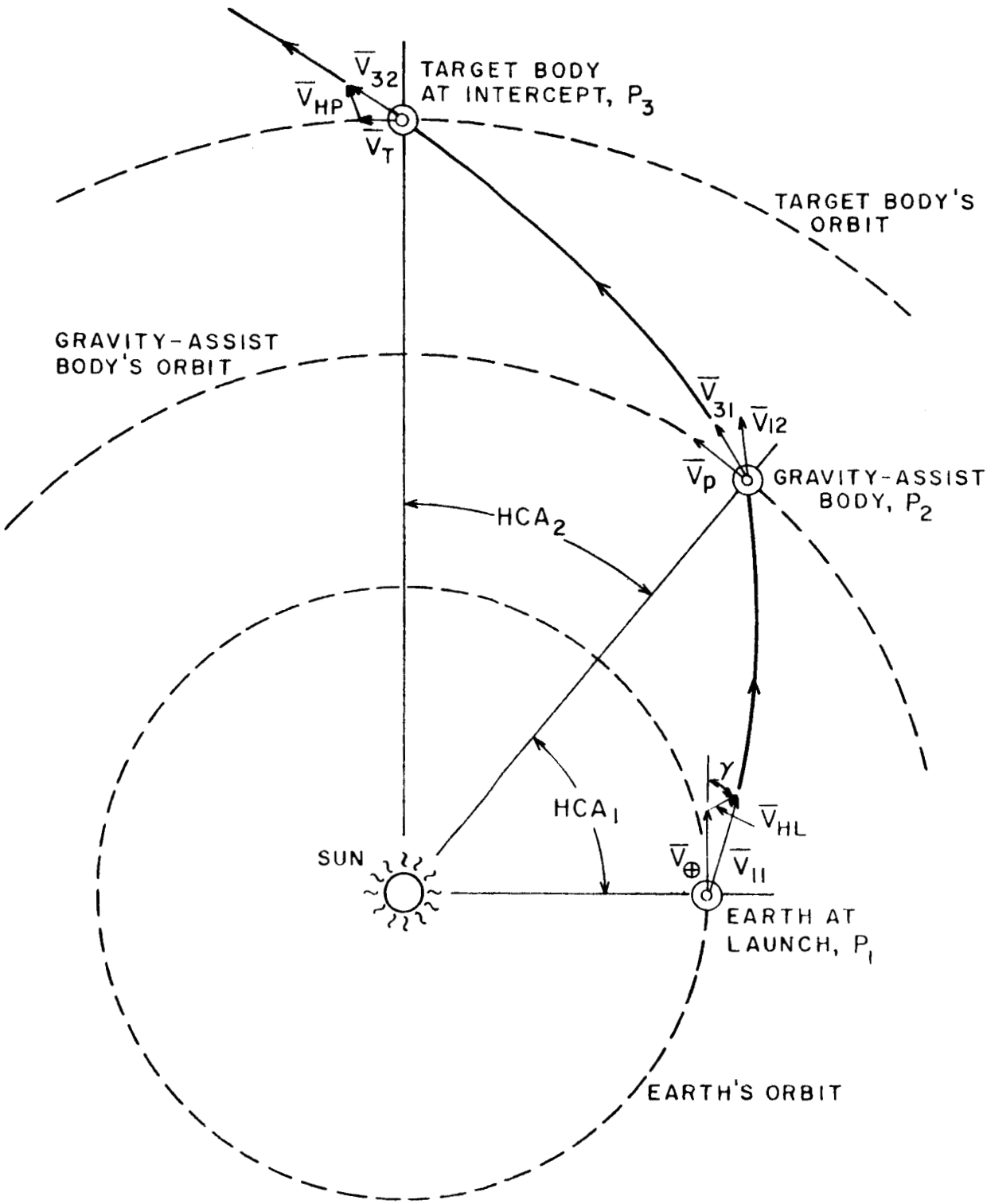

FIGURE 1. 2-D HELIOCENTRIC GEOMETRY.

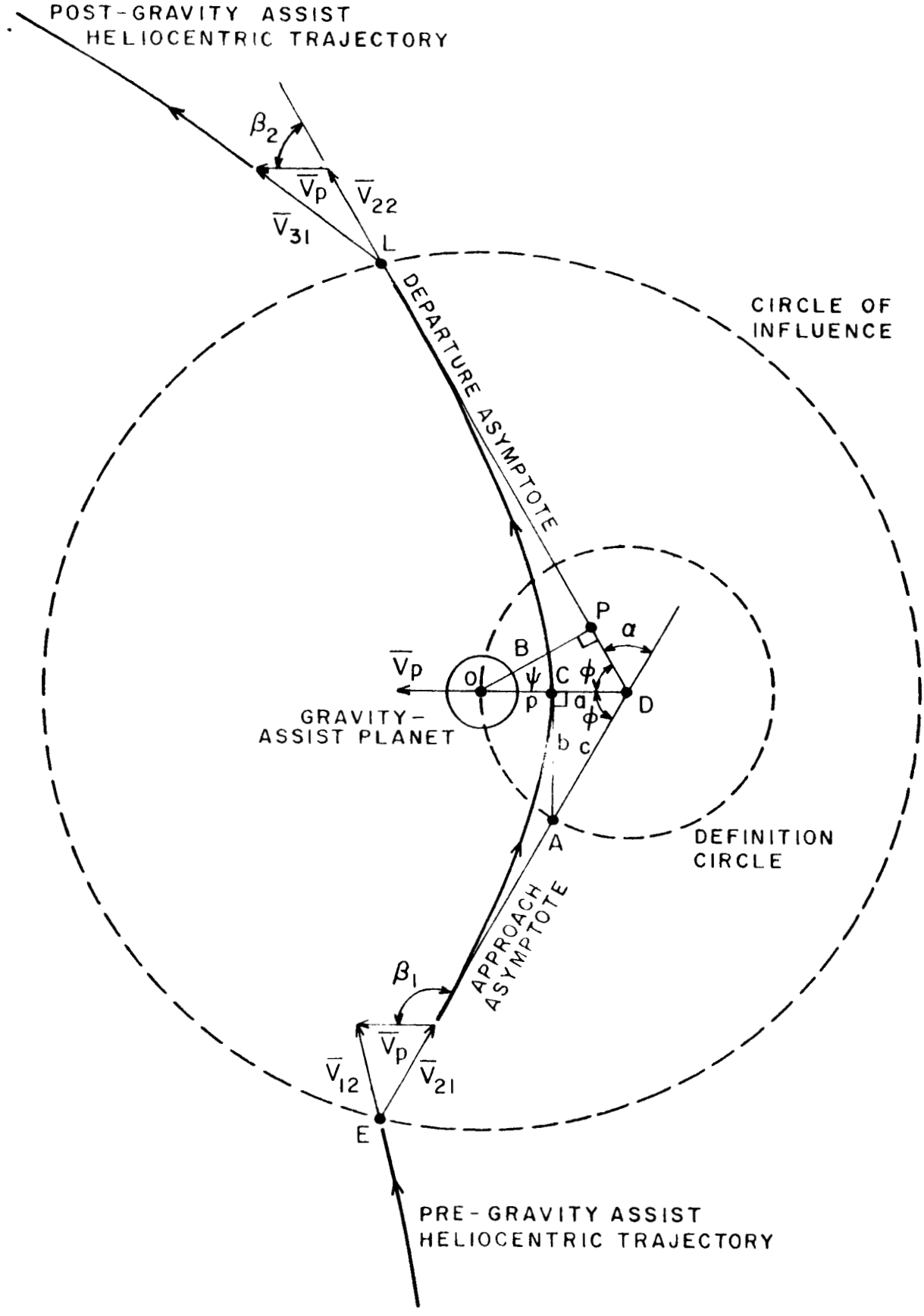

FIGURE 2. 2-D GRAVITY-ASSIST GEOMETRY.

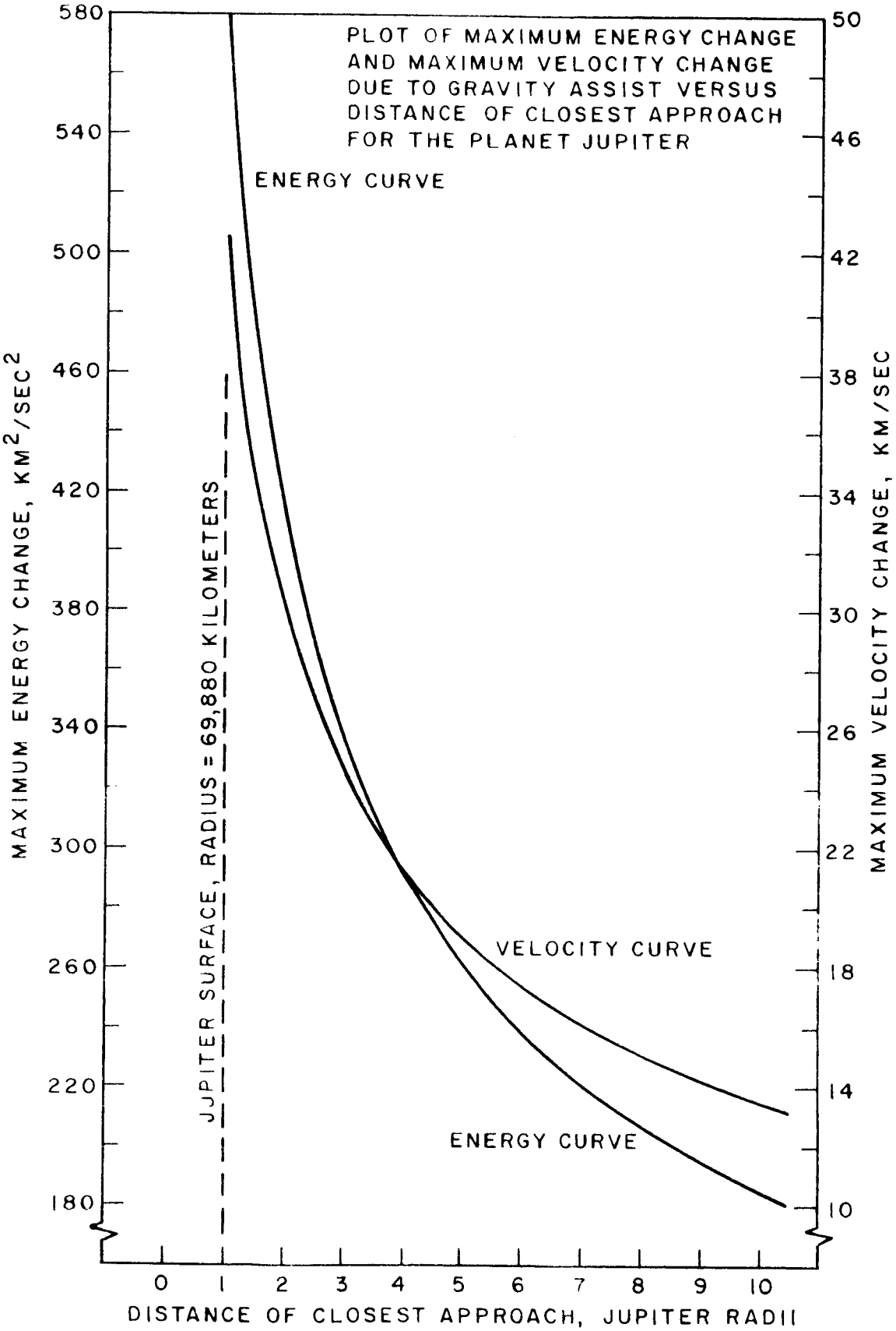

FIGURE 3. MAXIMUM VELOCITY AND ENERGY CHANGES: JUPITER.

IIT RESEARCH INSTITUTE

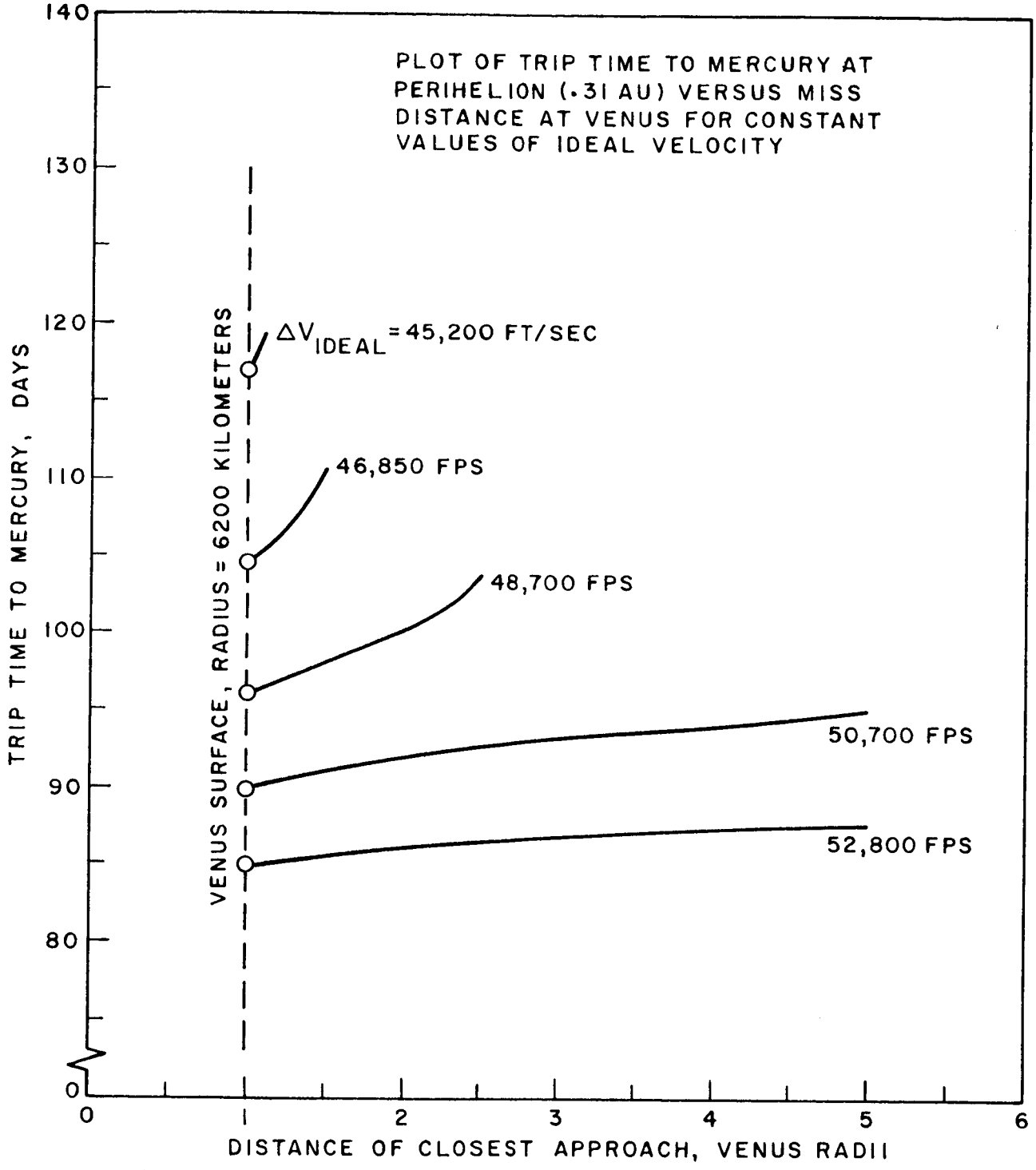

FIGURE 4. "DATA" GRAPH: EARTH-VENUS-MERCURY (0.31 AU).

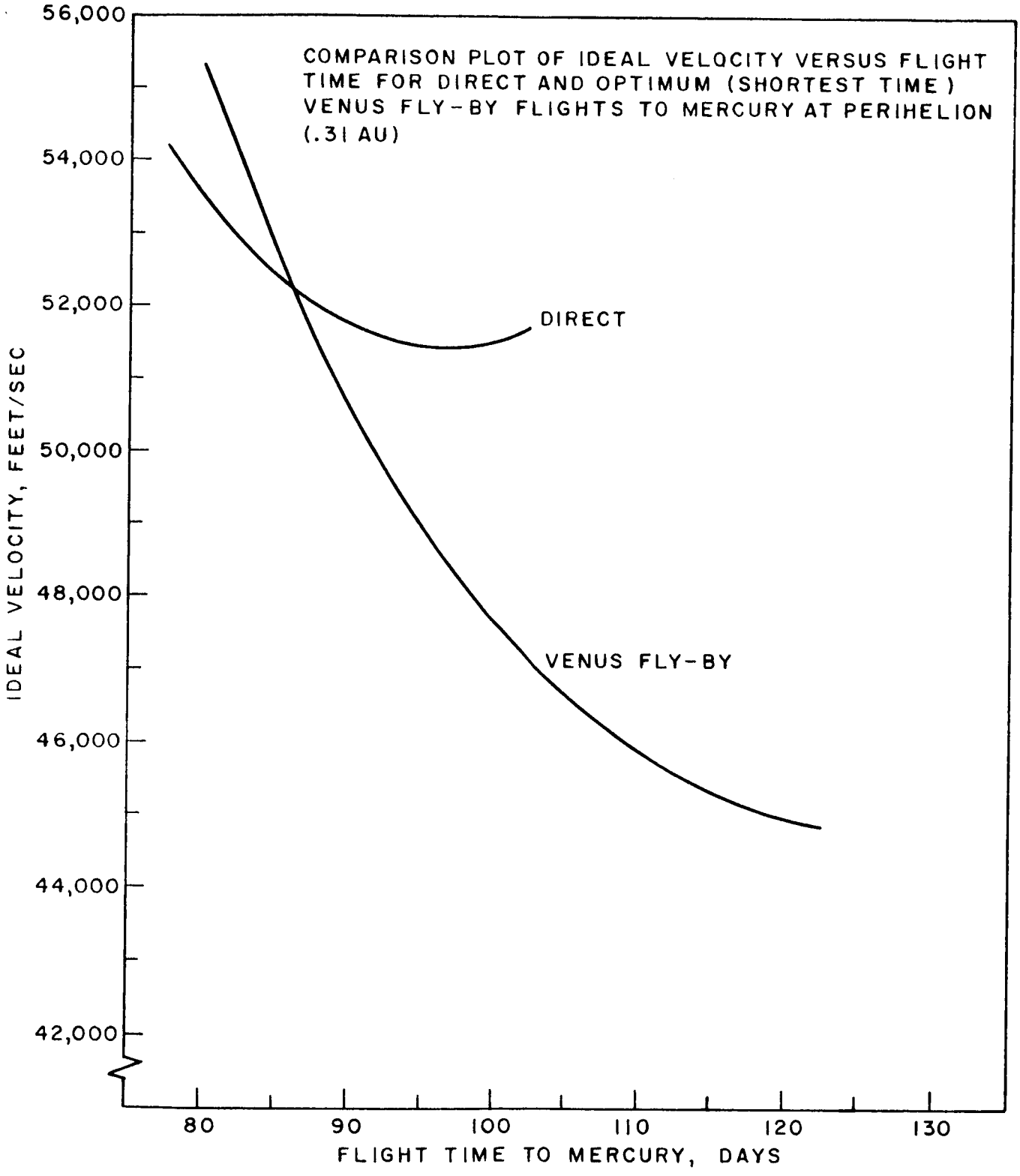

FIGURE 5. "MINIMUM TIME" GRAPH: EARTH-VENUS-MERCURY (0.31 AU).

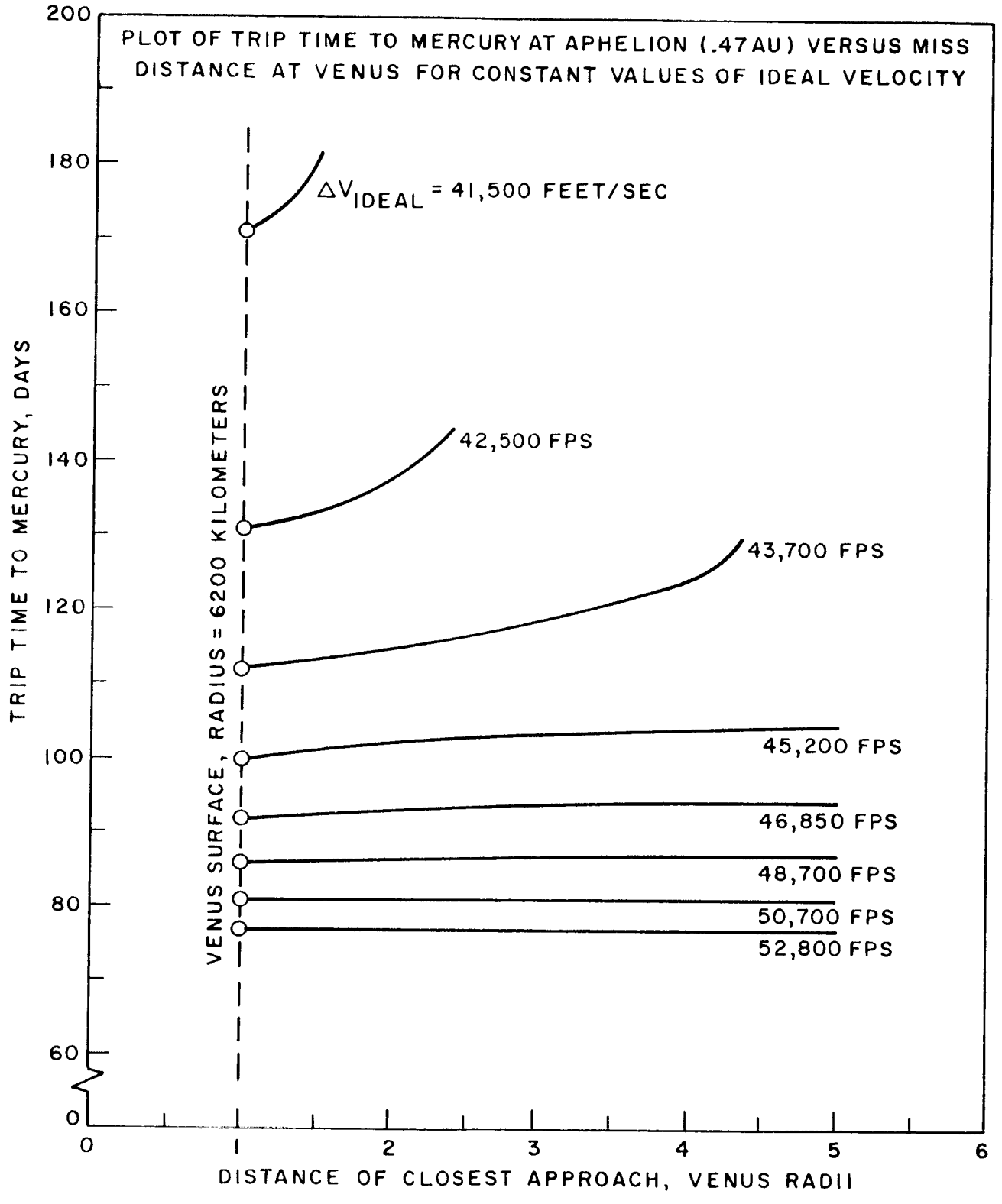

FIGURE 6. "DATA" GRAPH: EARTH-VENUS-MERCURY (0.47 AU).

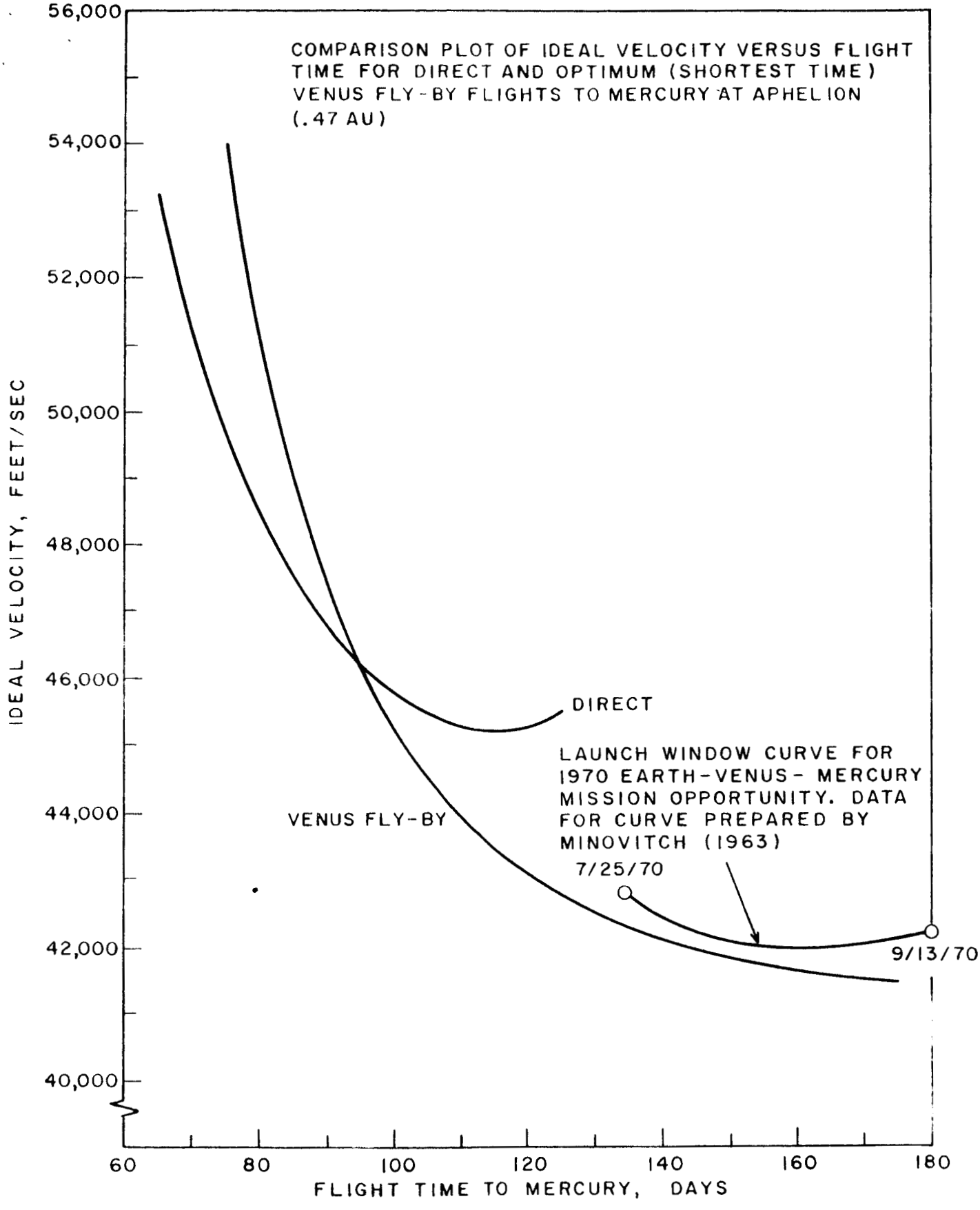

FIGURE 7. "MINIMUM TIME" GRAPH: EARTH-VENUS-MERCURY (0.47 AU).

III RESEARCH INSTITUTE

MERCURY PROBE VIA VENUS

TRAJECTORY DATA:

LAUNCH DATE, AUGUST 1970
IDEAL VELOCITY = 41,950 FEET/SEC
TIME TO VENUS = 100 DAYS
VENUS APPROACH VELOCITY = 7.1 KM/SEC
VENUS CLOSEST APPROACH = 1.66 VENUS RADII
TOTAL TRIP TIME = 160 DAYS
MERCURY APPROACH VELOCITY = 9.2 KM/SEC
MAXIMUM COMMUNICATION DISTANCE = 1.15 AU
EQUIVALENT DV AT VENUS = 5.48 KM/SEC

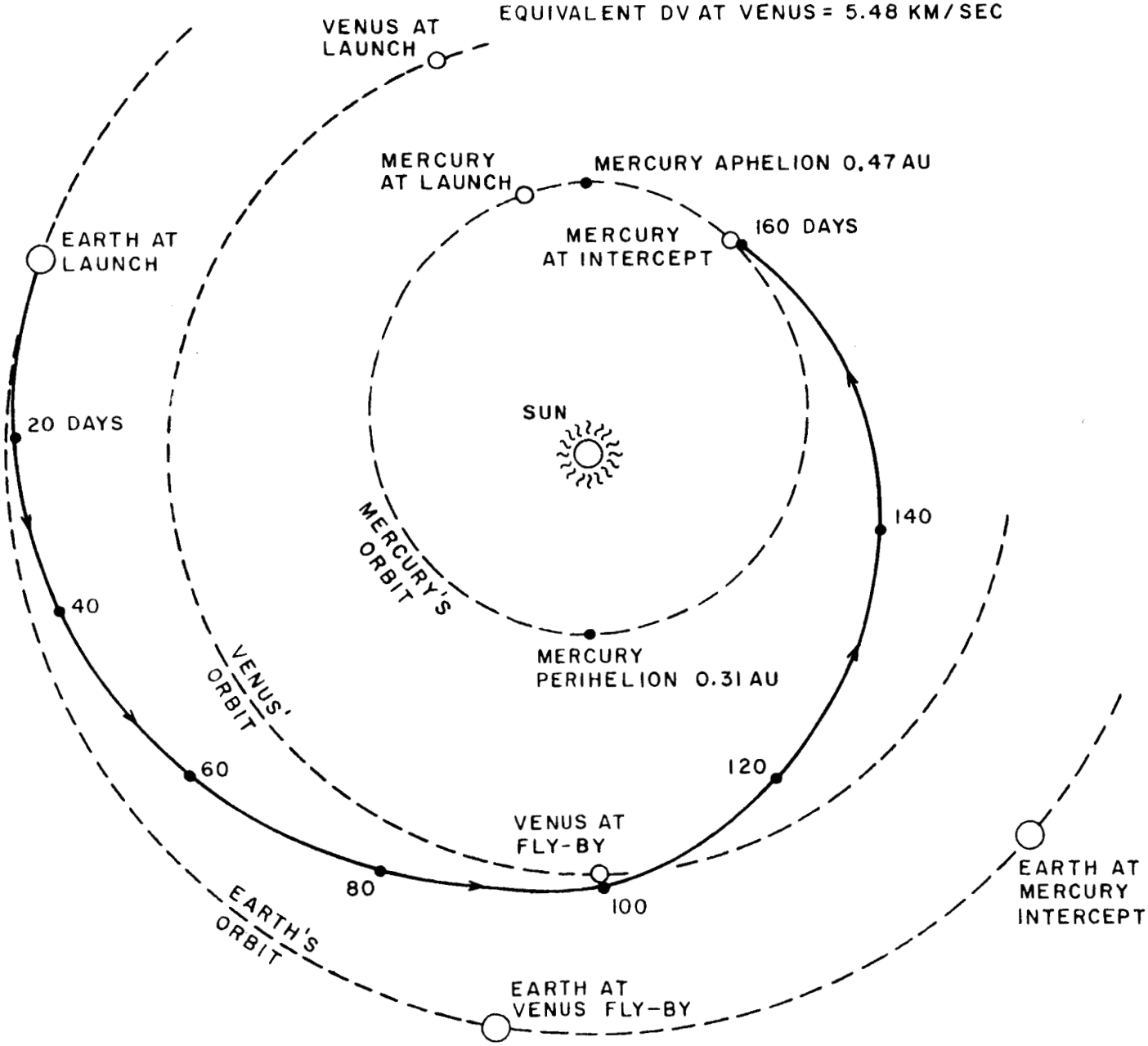

FIGURE 8. EARTH-VENUS-MERCURY MISSION ILLUSTRATION.

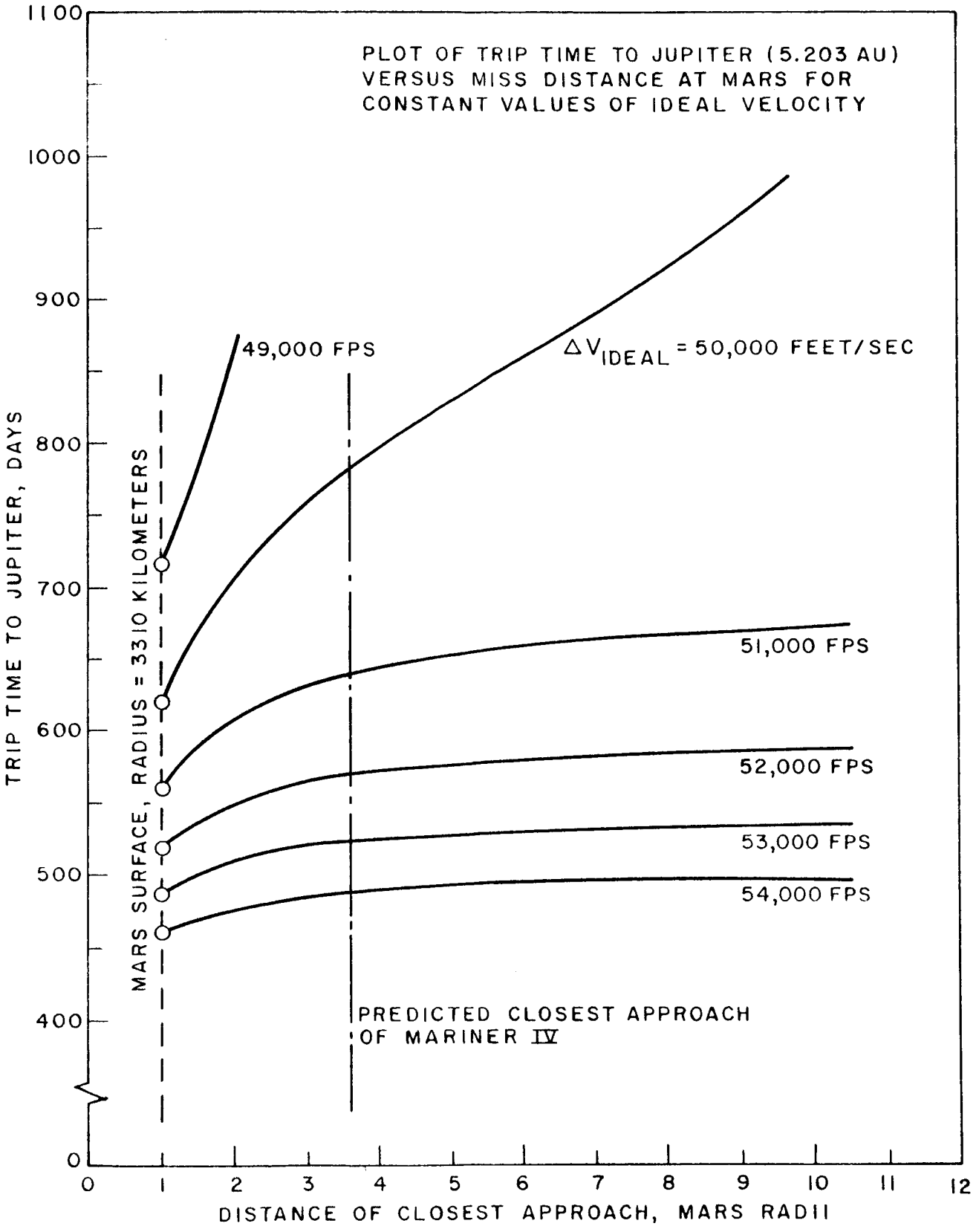

FIGURE 9. "DATA" GRAPH: EARTH-MARS-JUPITER.
IIT RESEARCH INSTITUTE

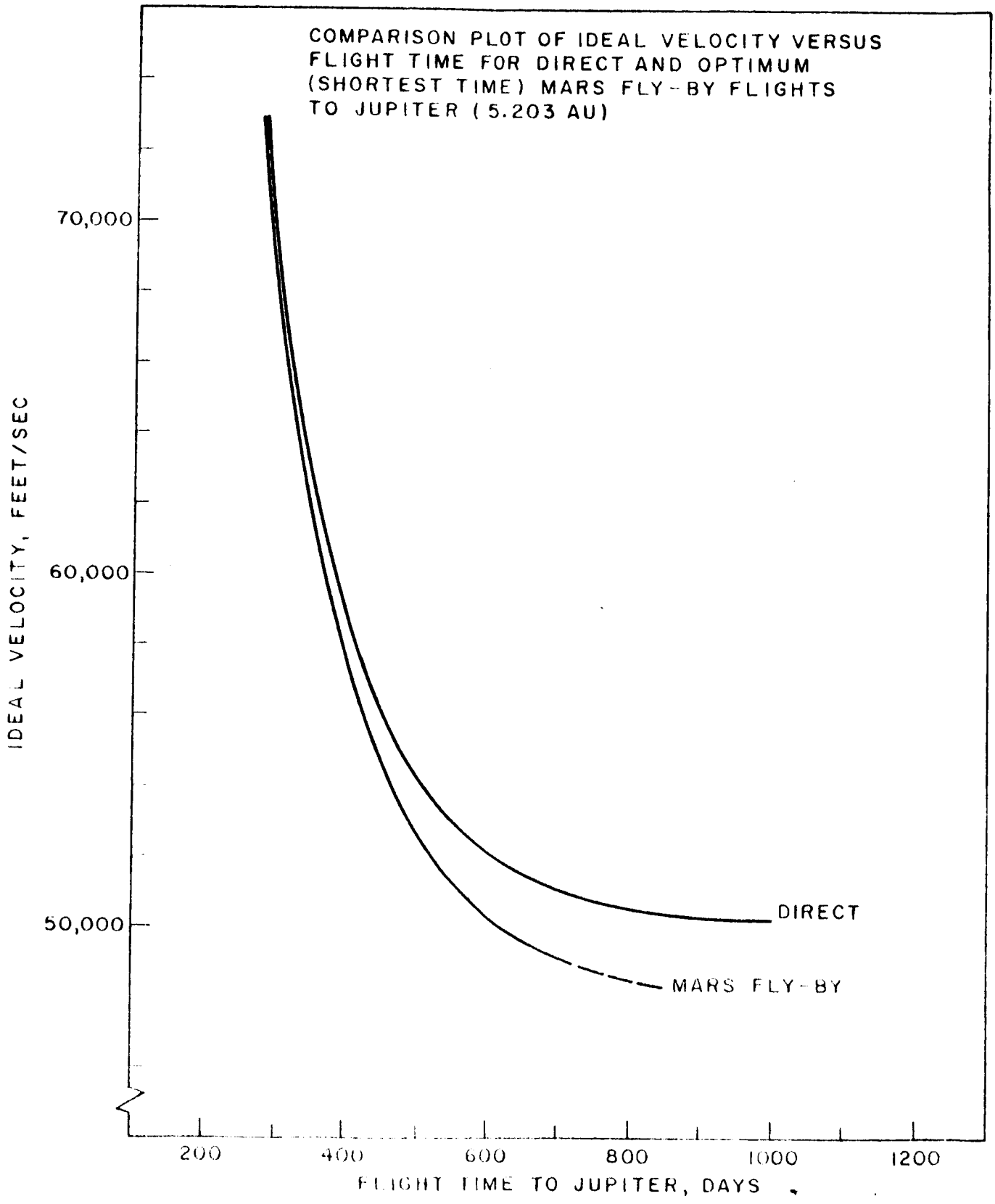

FIGURE 10. "MINIMUM TIME" GRAPH: EARTH-MARS-JUPITER.

IIT RESEARCH INSTITUTE

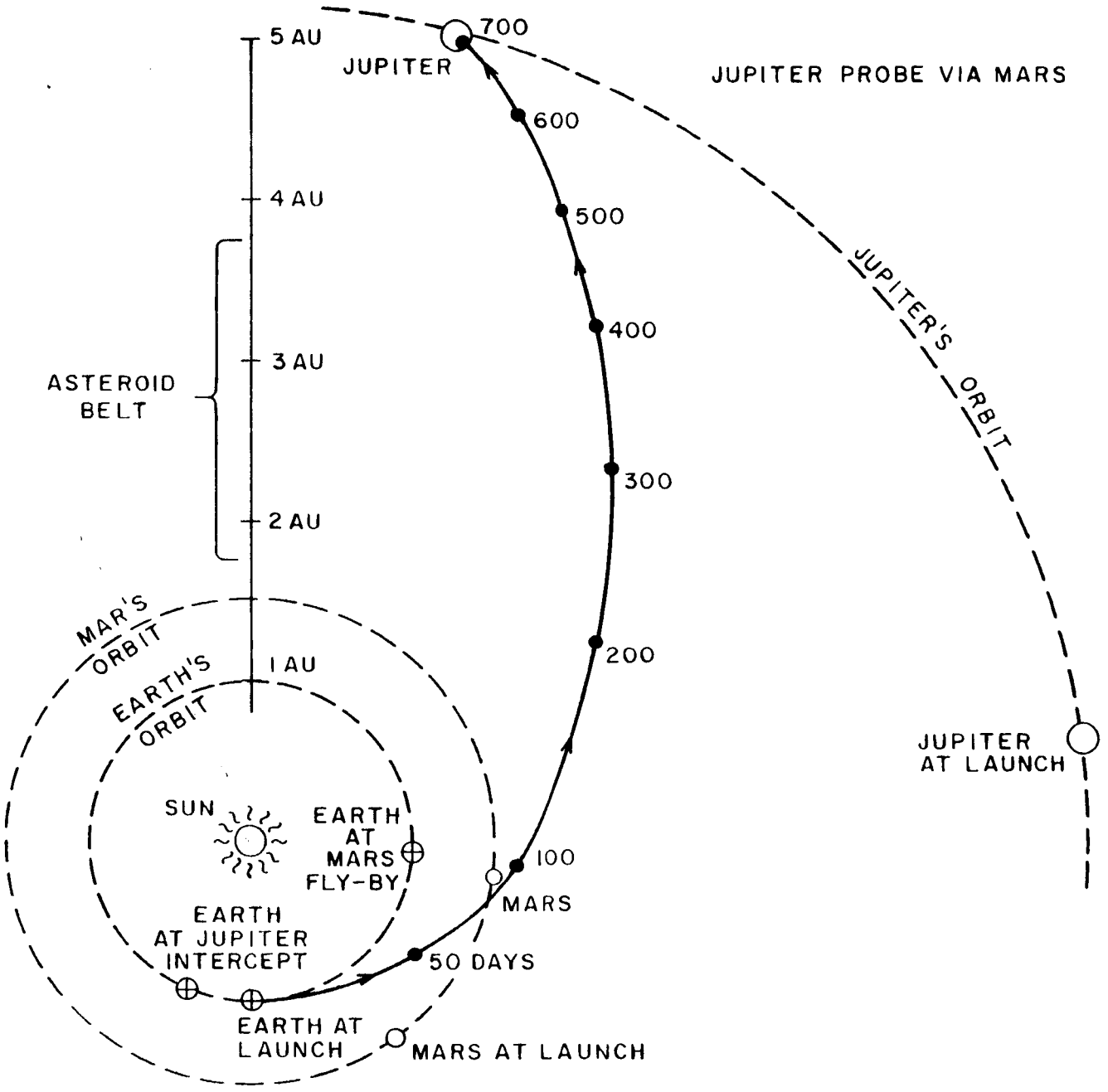

TRAJECTORY DATA:

LAUNCH DATE, MARCH 2, 1984
IDEAL VELOCITY = 50,000 FEET/SEC
MARS APPROACH VELOCITY = 14.9 KM/SEC
MARS CLOSEST APPROACH = 2 MARS RADII
JUPITER APPROACH VELOCITY = 7.6 KM/SEC
FLIGHT TIME TO JUPITER = 706 DAYS
MAXIMUM COMMUNICATION DISTANCE = 6.2 AU
EQUIVALENT DV AT MARS = 1.6 KM/SEC

FIGURE 11. EARTH-MARS-JUPITER MISSION ILLUSTRATION.
IIT RESEARCH INSTITUTE

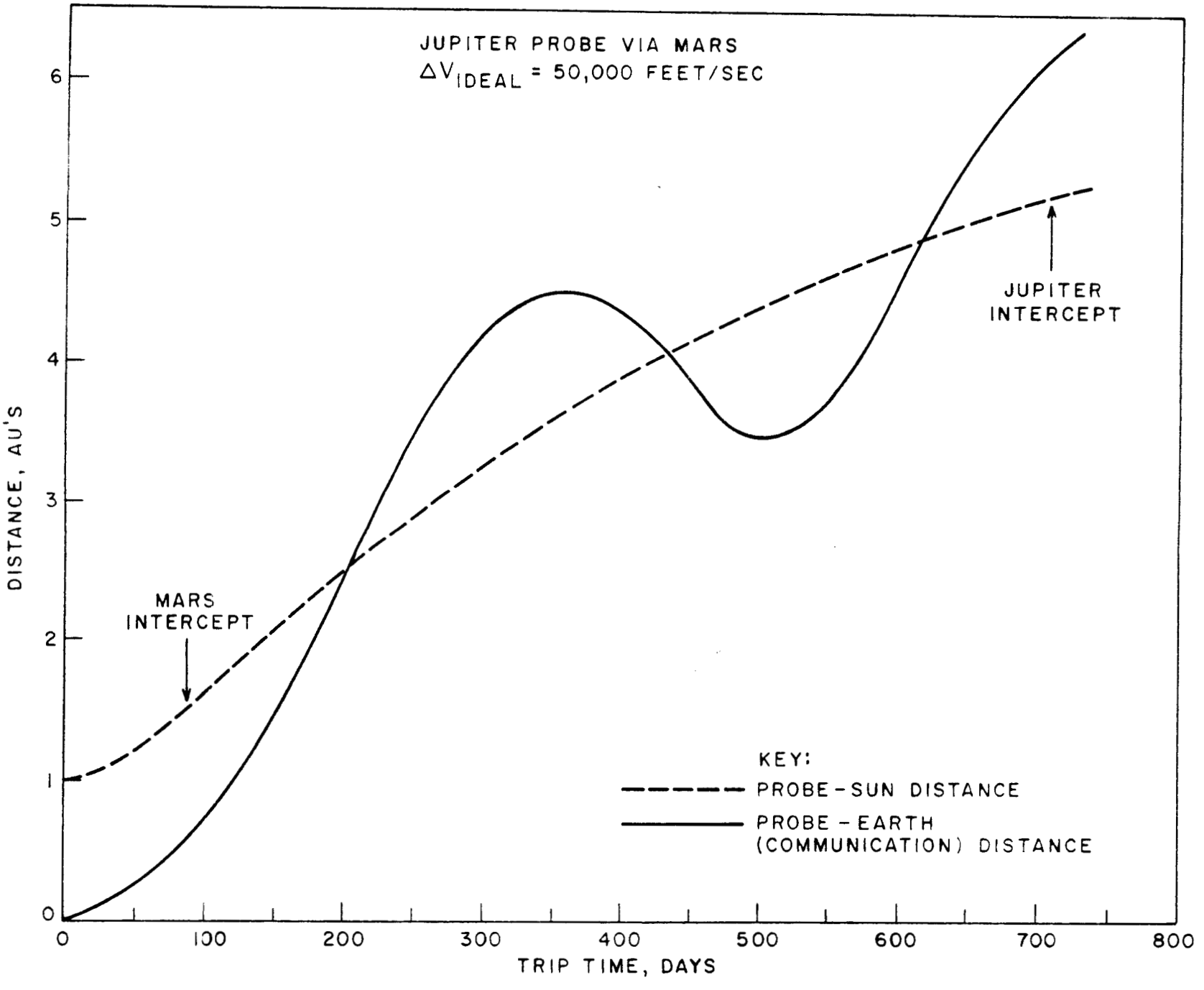

FIGURE 12. DISTANCE PLOT: EARTH-MARS-JUPITER MISSION.

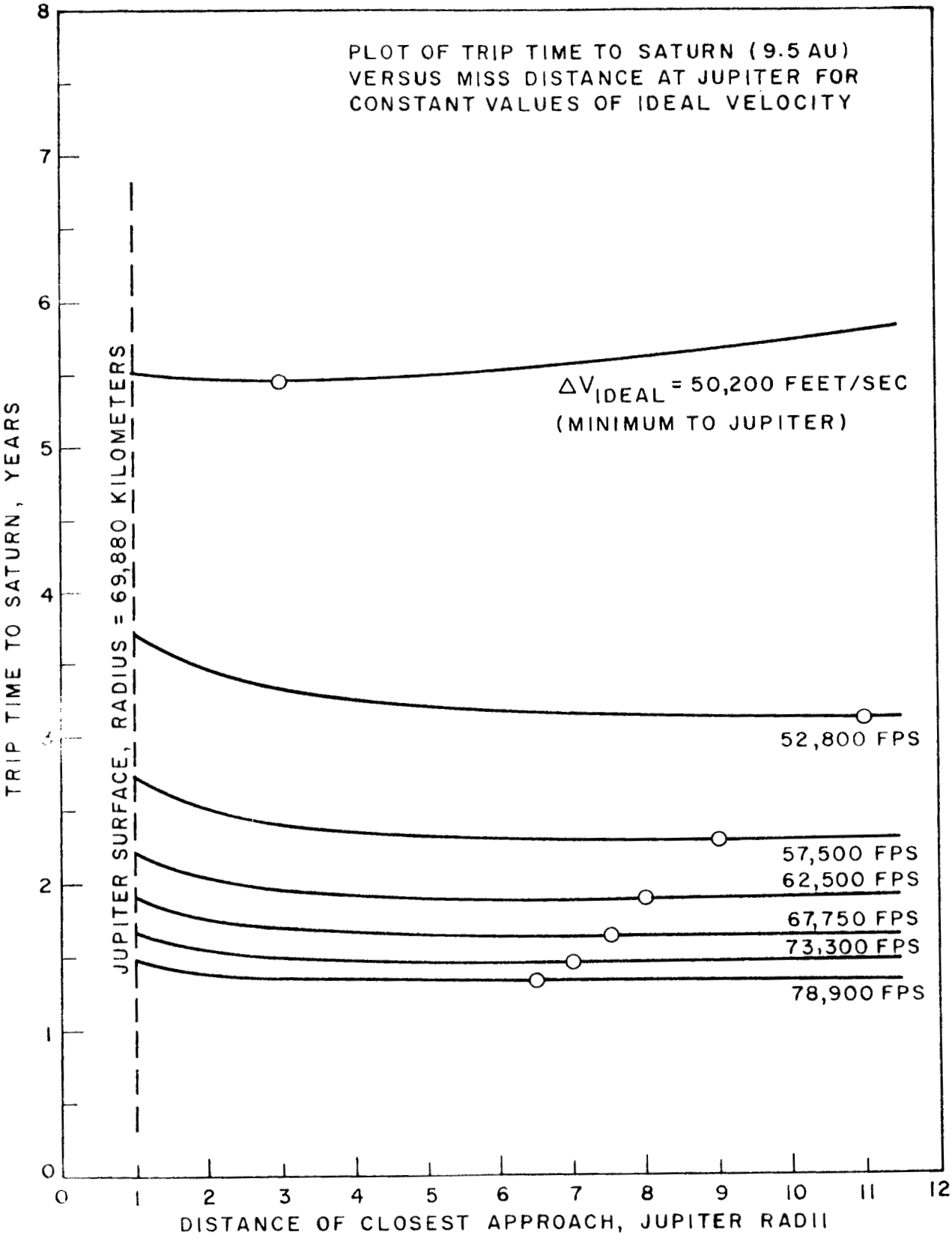

FIGURE 13. "DATA" GRAPH: EARTH - JUPITER - SATURN.

III RESEARCH INSTITUTE

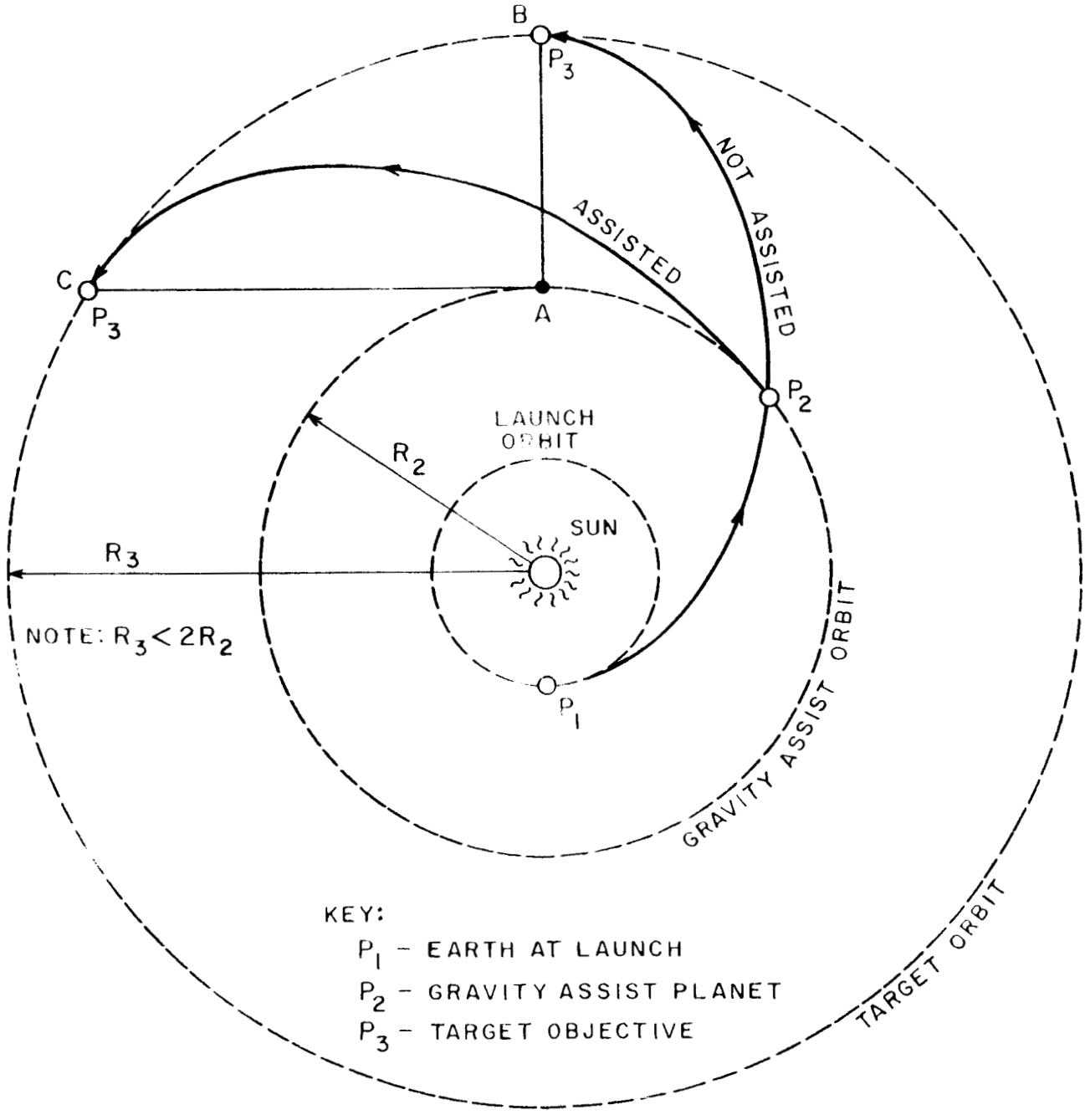

FIGURE 14. TRAJECTORY GEOMETRY FOR MISS DISTANCE TRADE-OFF CHARACTERISTIC AT P_2.

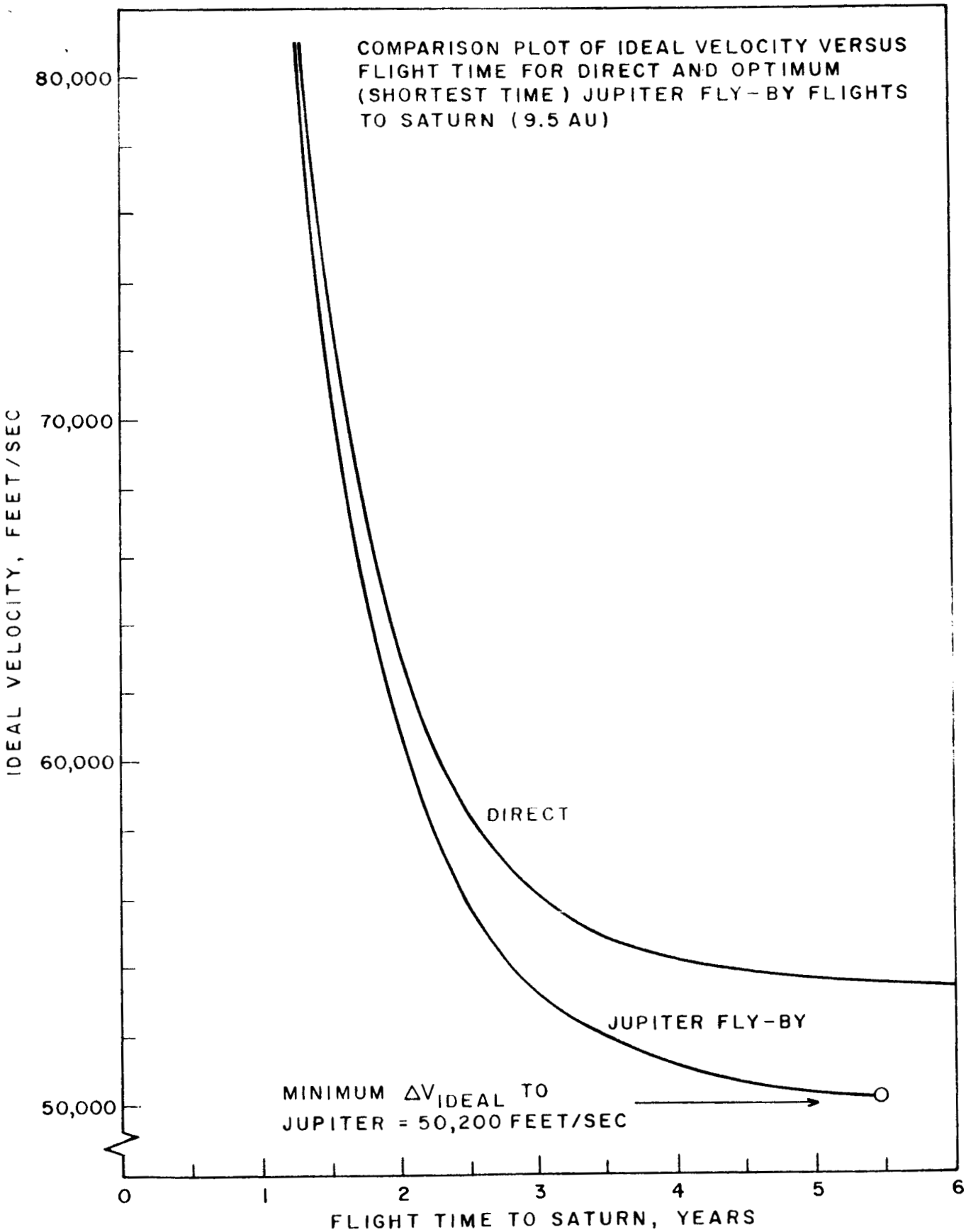

FIGURE 15. "MINIMUM TIME" GRAPH: EARTH-JUPITER-SATURN.

IIT RESEARCH INSTITUTE

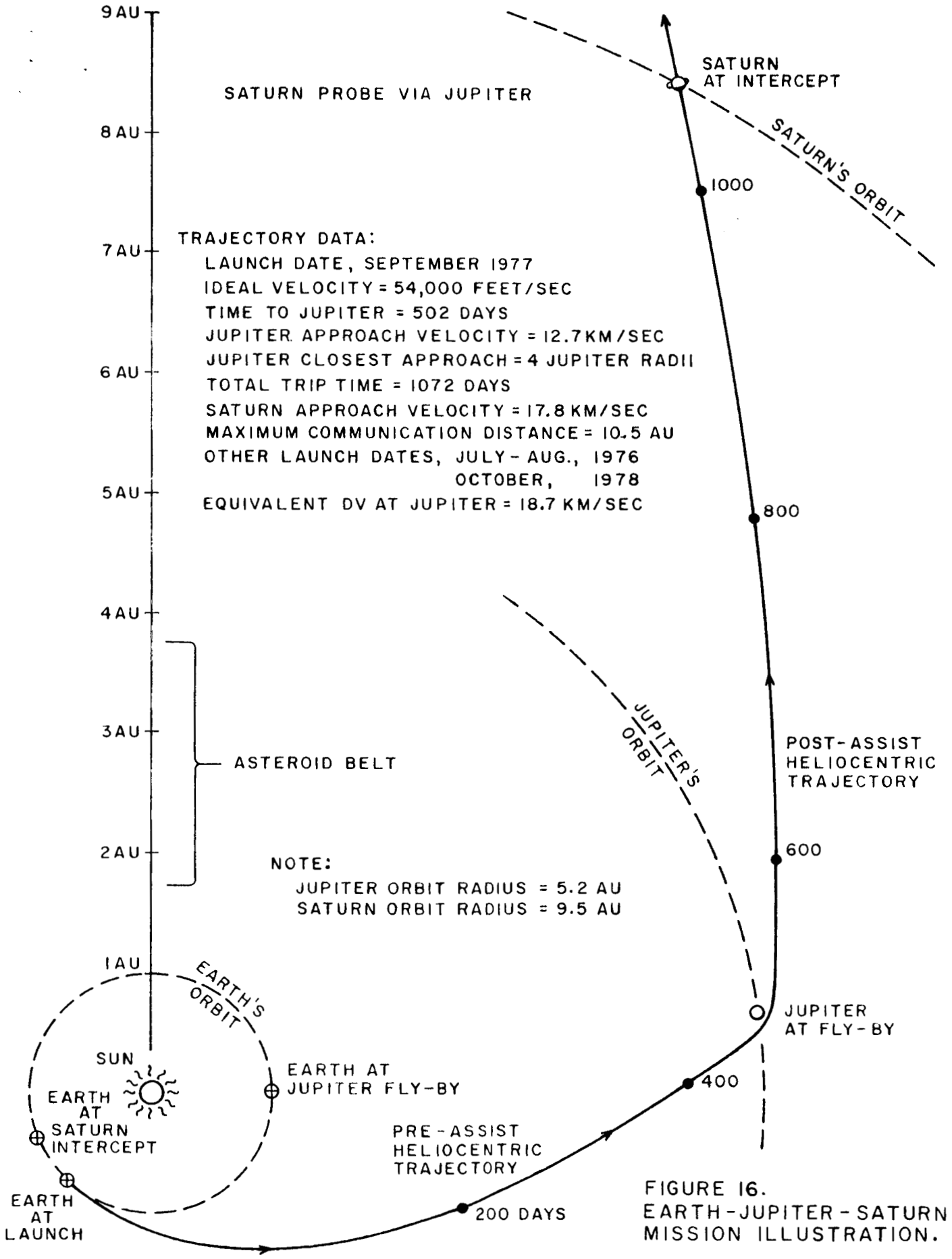

FIGURE 16.
EARTH-JUPITER-SATURN
MISSION ILLUSTRATION.

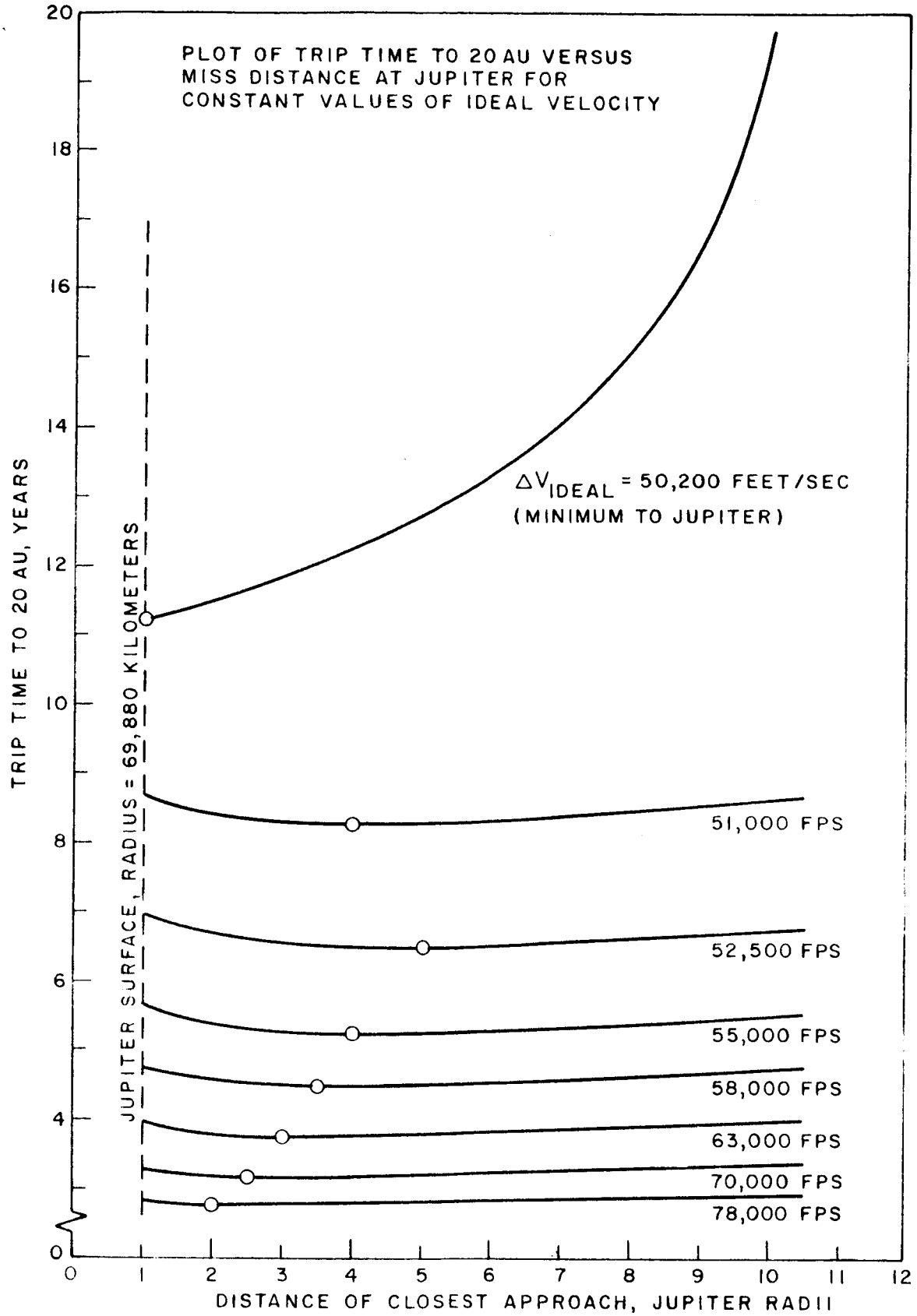

FIGURE 17. "DATA" GRAPH: EARTH - JUPITER - 20 AU.

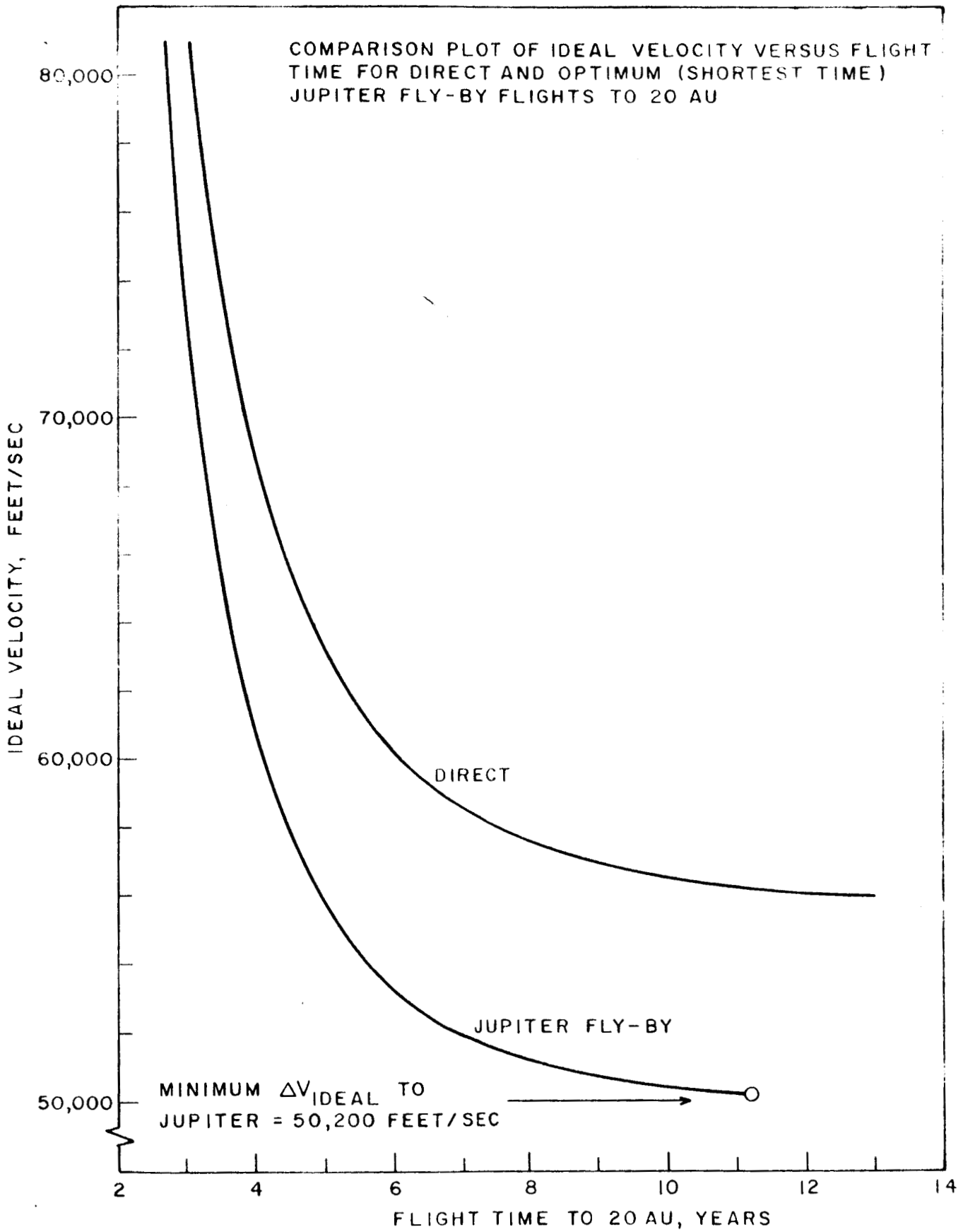

FIGURE 18. "MINIMUM TIME" GRAPH: EARTH-JUPITER - 20 AU.
IIT RESEARCH INSTITUTE

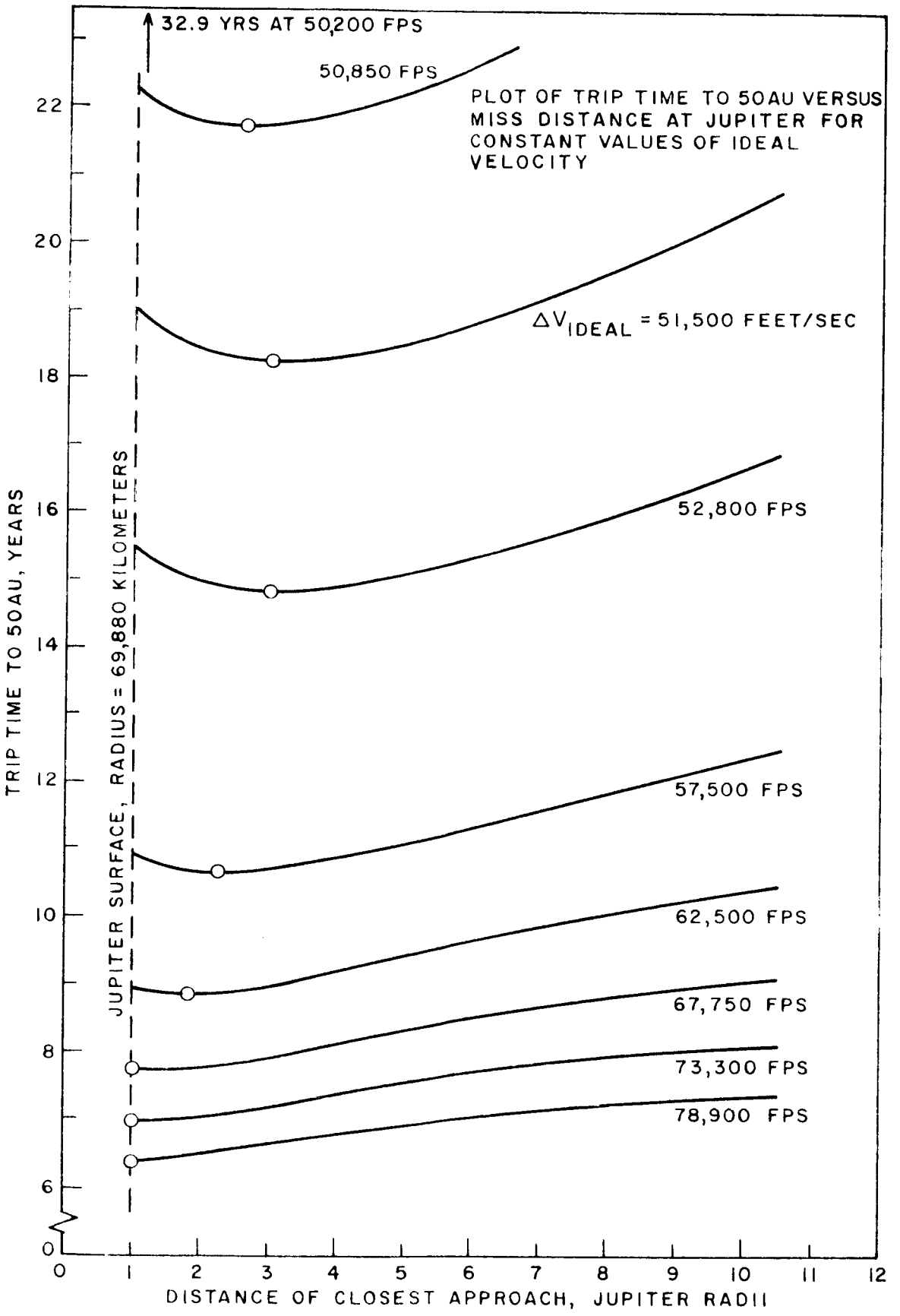

FIGURE 19. "DATA" GRAPH: EARTH-JUPITER-50 AU.

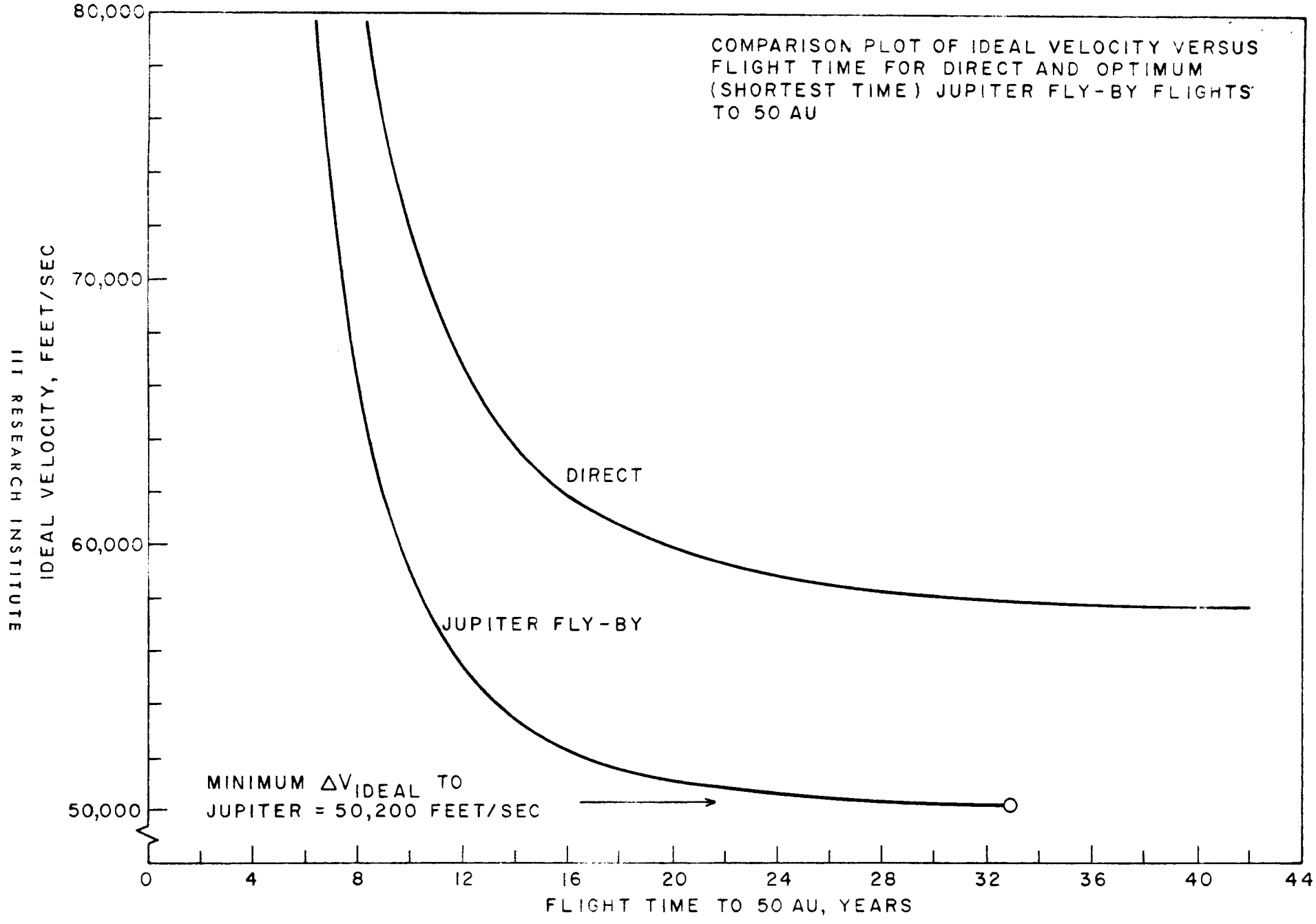

FIGURE 20. "MINIMUM TIME" GRAPH: EARTH-JUPITER - 50 AU.

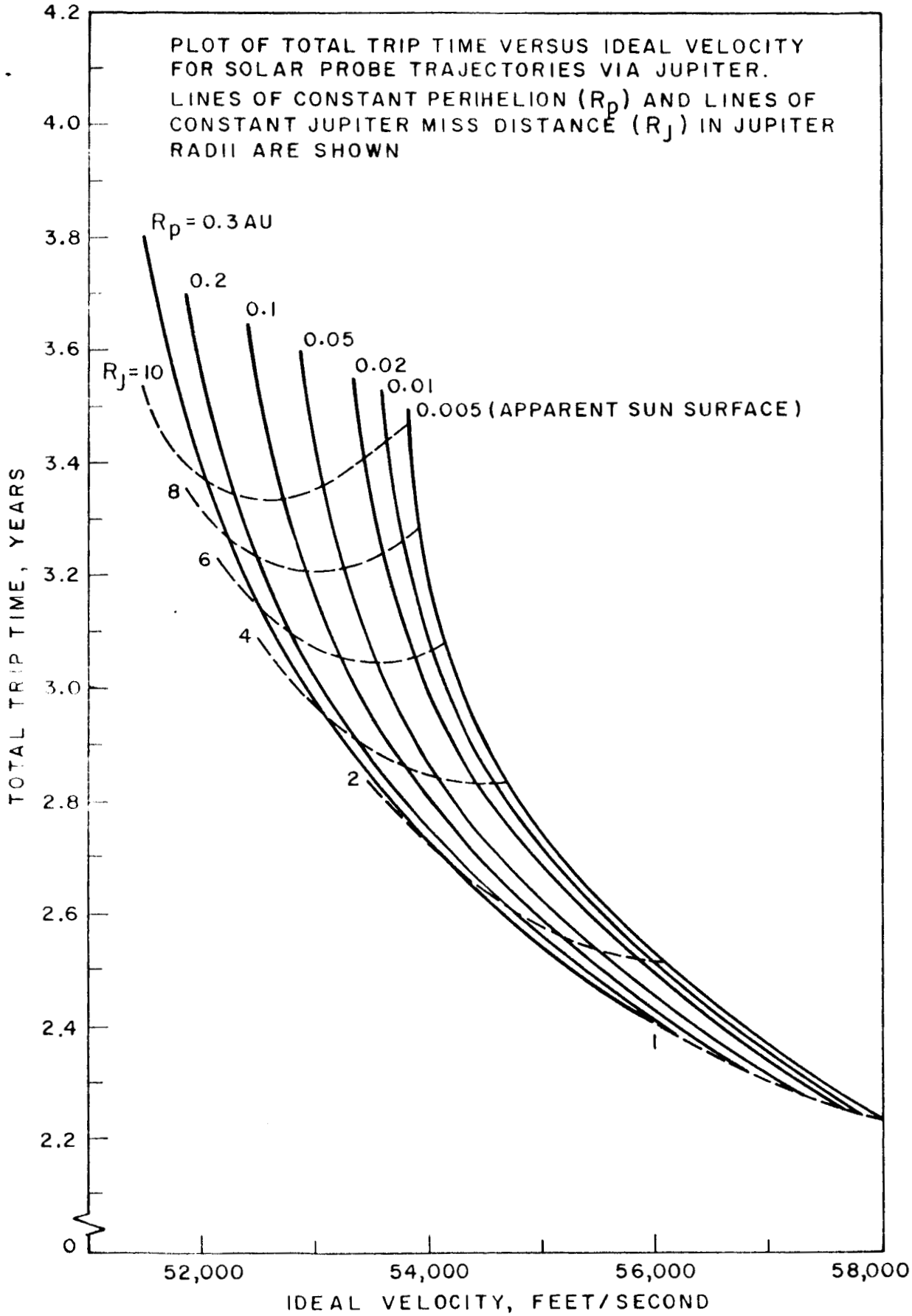

FIGURE 21. EARTH-JUPITER-SOLAR PROBE MISSION SELECTION GRAPH.

IIT RESEARCH INSTITUTE

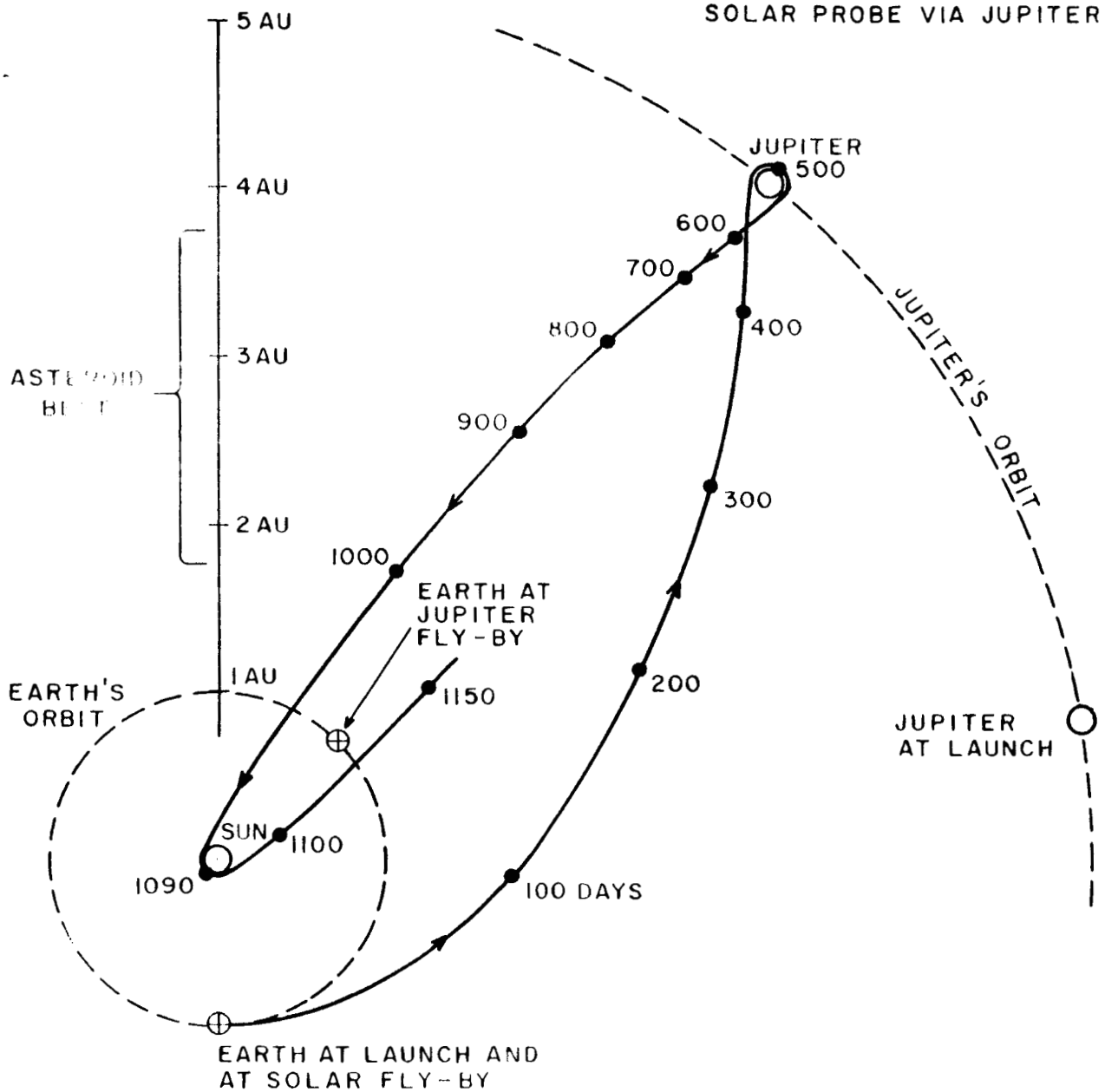

LAUNCH DATES:

JAN 1 1970
FEB 4 1971
MAR 10 1972
APR 14 1973
MAY 19 1974
JUN 23 1975
JUL 27 1976
AUG 31 1977
OCT 5 1978
NOV 9 1979

TRAJECTORY DATA:

IDEAL VELOCITY = 54,000 FEET/SEC
JUPITER APPROACH VELOCITY = 12.7 KM/SEC
JUPITER CLOSEST APPROACH = 5.3 JUPITER RADII
SUN CLOSEST APPROACH = 0.02 AU
VELOCITY AT 0.02 AU = 298 KM/SEC
FLIGHT TIME TO 0.02 AU = 3 YEARS
MAXIMUM COMMUNICATION DISTANCE = 5.5 AU
EQUIVALENT DV AT JUPITER = 17.5 KM/SEC

FIGURE 22. EARTH-JUPITER-SOLAR PROBE MISSION ILLUSTRATION.

IIT RESEARCH INSTITUTE

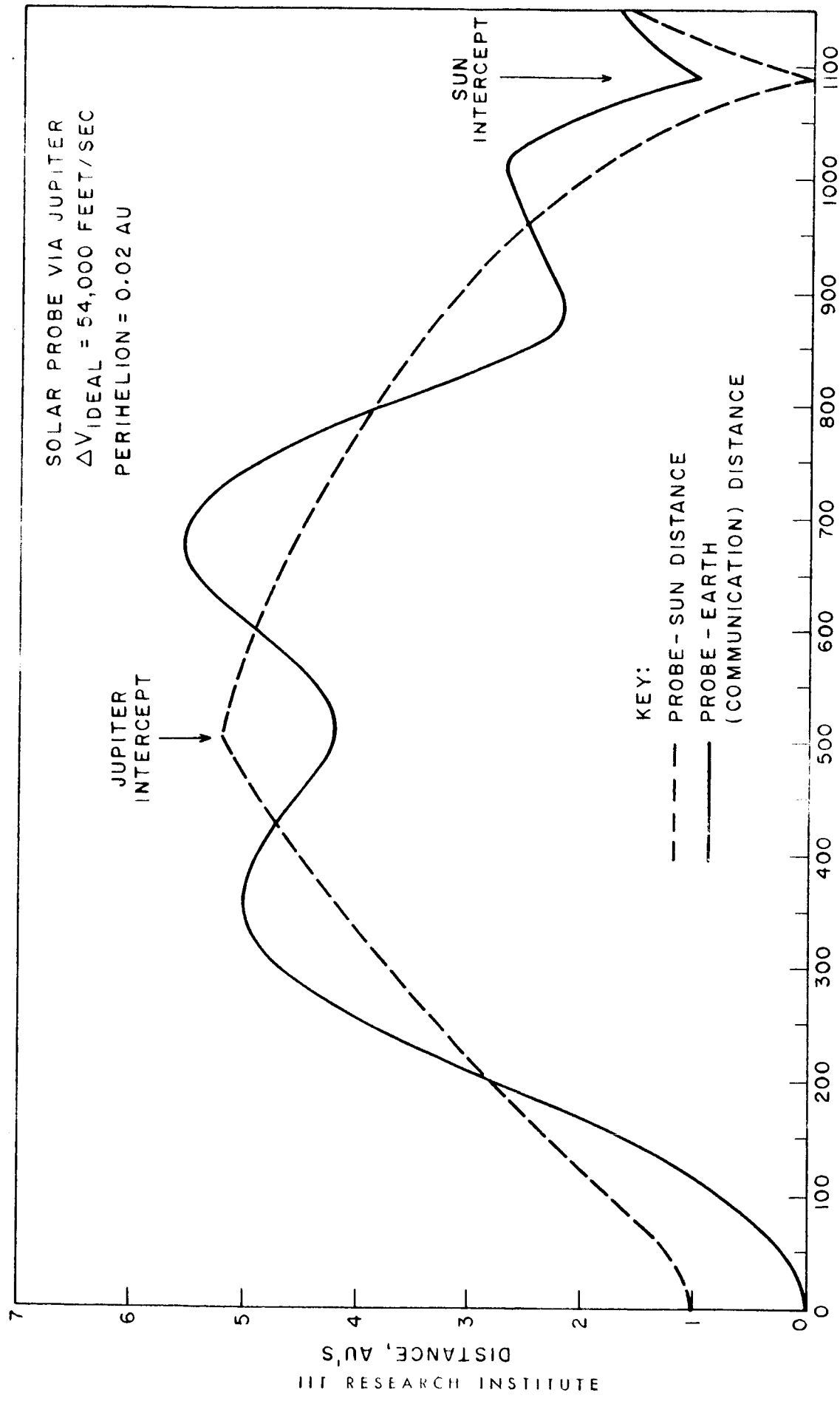

FIGURE 23. DISTANCE PLOT: EARTH-JUPITER-SOLAR PROBE.

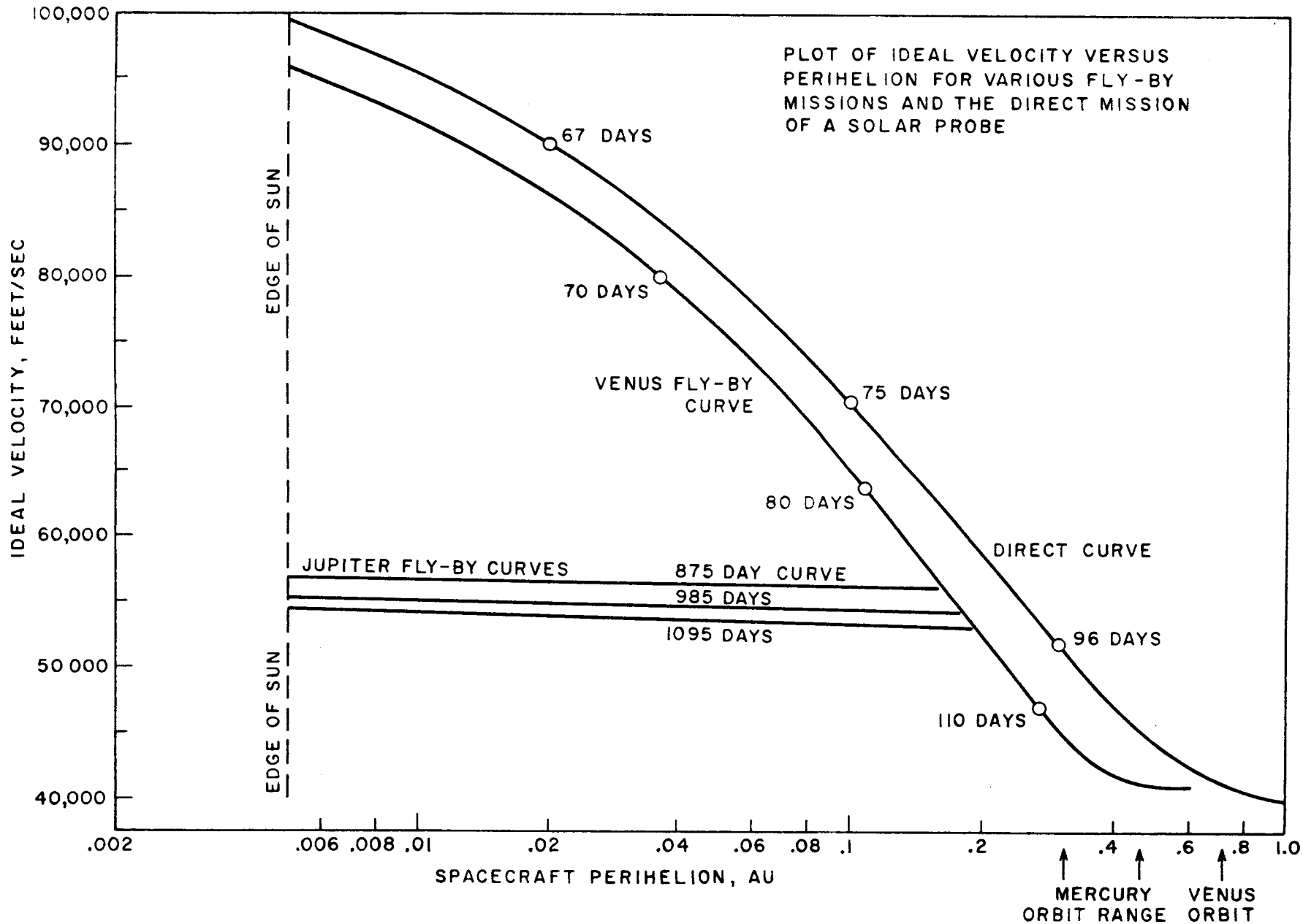

FIGURE 24. SOLAR PROBE MISSION COMPARISON PLOT.